FREE RADICAL POLYMERIZATIONS ASSOCIATED WITH THE TROMMSDORFF EFFECT UNDER SEMIBATCH REACTOR CONDITIONS : ON-LINE INFERENTIAL STATE ESTIMATION

A Thesis Submitted
in Partial Fulfilment of the Requirements
for the Degree of
Master of Technology

by

G. B. Bhargava Ram

to the

DEPARTMENT OF CHEMICAL ENGINEERING
INDIAN INSTITUTE OF TECHNOLOGY, KANPUR
July 1996.

CERTIFICATE

This is to certify that the present work entitled, FREE RADICAL POLYMERIZATIONS ASSOCIATED WITH THE TROMMSDORFF EFFECT UNDER SEMIBATCH REACTOR CONDITIONS : ON-LINE INFERENTIAL STATE ESTIMATION, by *G.B.Bhargava Ram* has been carried out under our supervision and that this work has not been submitted elsewhere for a degree.

Prof. D.N.Saraf,
Professor,
Department of Chemical Engg.
IIT, Kanpur.
July,96

Prof. S.K.Gupta,
Professor,
Department of Chemical Engg.
IIT, Kanpur.

ABSTRACT

A moving-horizon inferential state-estimation technique is described which uses simulated 'experimental' data (obtained by adding random fluctuations to model results) on temperature and viscosity to study *bulk* polymerization of free radical systems. The short-term predictive capability of this technique is found to be quite good (except for the case when the curve-fitting horizon lies just before the gel-effect region, and does not include even a single 'experimental' point from this region). A considerable amount of ringing (oscillations between the lower and upper bounds) is observed in the values of the estimated parameters. The ringing can be reduced significantly by narrowing down the range of parameter values, or by taking 'experimental' data which are spaced further apart. The long-term predictions of the model using the estimated parameters may or may not be excellent, depending on the 'local' values of the parameters. Because of this, periodic use of state-variable estimation followed by the determination of the optimal temperature history in the future, could be a feasible strategy for experimental on-line optimizing control of bulk free-radical polymerizations which exhibit significant amounts of the Trommsdorff effect.

CONTENTS

ACKNOWLEDGEMENT

Truly speaking, I had one of the most memorable experiences at IIT Kanpur working under our **SIRS**, Dr D. N. Saraf and Dr S. K. Gupta. While carrying out the research, the weekly meetings held with Dr Gupta and Dr Saraf, helped me to interact more effectively and freely to discuss and sort out the problems. I woe them a lot for the patience they had to guide me in solving the problems and inspiring me to put much more efforts. I don't know whether I could be able to meet their expectations in pursuing my duties. I feel very happy for having the opportunity to work under them. I extend my sincere regards to them.

I offer my sincere thanks to my labmates, Mankarji, Garg, Pallab, Mitra, Sajith, Kohli, Verma and Sasank Raha, who helped me towards completing the work in time and made me feel very comfortable in our lab.

I am very much thankful to my friends and classmates, Prasad, Chakri, Sastry, Poorna, Anil, C. V. Rao and Chavan, for making my stay at IIT Kanpur a memorable one. I feel fortunate enough for having friends like Kali and Murthy, who are with me all the time and constantly inspiring me to work in a better way. I offer my regards to my seniors, SVRao, Khr and Pavitra.

Finally, my eternal gratitude goes to my parents and brothers for their love and affection.

LIST OF FIGURES

Variation of a_1 - d_1 for the curve-fitting of non-randomized, isothermal (50 ^{o}C) data shown in Fig. 14. Values of N_1 and N_3 for the various cases are given in Table 3. Scales for cases A and C are indicated on the left, while for cases B and D are on the right hand side.

LIST OF TABLES

NOMENCLATURE

a	parameter in the Mark-Houwink equation
a_1-a_3	parameters in correlation of θ_t
b	parameter in the Lyons-Tobolsky equation, m^3 kg^{-1}
b_1-b_3	parameters in correlation of θ_p
C_{polym}	concentration of polymer, kg m^{-3}
c_1-c_3	parameters in correlation of θ_f
D_n	dead polymer molecule having n repeating units
d_1, d_2	parameters in Equation for k_H
E	objective function
E_d, E_p, E_t	activation energies for initiation, propagation and termination in absence of gel or glass effects, kJ mol^{-1}
f	initiator efficiency
f_o	initiator efficiency in the limiting case of zero diffusional resistance
I	initiator (AIBN)
$[I]_o$	initial molar concentration of initiator, mol m^{-3}
K	parameter in the Mark-Houwink equation, m^3 kg^{-1}
k_H	Huggins' constant, dimensionless
$k_d, k_f, k_i, k_p,$ k_s, k_{tc}, k_{td}	rate constants for the reactions in Table 1 at any time t, s^{-1} or m^3 $mol^{-1}s^{-1}$
k_t	$k_{tc} + k_{td}$
k_d^o, $k_{p,o}^o$, $k_{t,o}^o$	frequency factors for initiation, propagation and termination in absence of the gel and glass effects, s^{-1} or m^3 mol^{-1} s^{-1}

$k_{t,o}$, $k_{p,o}$ $k_{i,o}$	k_t, k_p and k_i in absence of gel and glass effects, $m^3\ mol^{-1}\ s^{-1}$
M	moles of monomer (MMA) in liquid phase, mol
M_{jp}	molecular weight of polymer jumping unit, kg mol^{-1}
M_n	number average molecular weight = $(MW_m)(\lambda_1+\mu_1)/(\lambda_o+\mu_o)$, kg mol^{-1}
M_w	weight average molecular weight = $(MW_m)(\lambda_2+\mu_2)/(\lambda_1+\mu_1)$, kg mol^{-1}
(MW_I), (MW_m), (MW_s)	molecular weights of pure initiator, monomer and solvent, kg mol^{-1}
N_1	number of points in the curve - fit horizon
N_2	number of points in the prediction horizon
N_3	number of data points to be deleted from the old curve-fit horizon
P_n	growing polymer radical having n repeat units
R	primary radical
R	universal gas constant, J mol^{-1} K^{-1}
R_{li}, R_{lm}, R_{ls}	rate of continuous addition of (liquid) initiator, monomer and solvent to reactor, mol s^{-1}
R_{vm}, R_{vs}	rate of evaporation of monomer or solvent, mol s^{-1}
S	solvent
S·	solvent radical
T	temperature of reaction mixture at time t, K
t	time, min
t_1	time at which state estimation is made, min

T	temperature of reaction mixture at time t, K
t	time, min
t_1	time at which state estimation is made, min
V_l	volume of liquid at time t, m^3
V_{fm}, V_{fp}, V_{fs}	fractional free volumes of monomer, polymer and solvent in reaction mixture
$\hat{V}_i^*$, $\hat{V}_m^*$, $\hat{V}_p^*$, $\hat{V}_s^*$	specific critical hole free volumes of initiator, monomer, polymer and solvent, $m^3\ kg^{-1}$
$\underset{\sim}{x}$	vector representing state variables
x_m	monomer conversion (molar) at time t

Greek Letters

γ	overlap factor
ζ_m, ζ_{m1}	net monomer added to the reactor
η	viscosity of the reaction mass, Pa-s
$[\eta]$	intrinsic viscosity, $m^3\ kg^{-1}$
η_{sol}	solvent (monomer) viscosity, Pa-s
θ_f, θ_p, θ_t	adjustable parameters in the model for cage, gel and glass effects, respectively, $m^3\ mol^{-1}$, s, s
λ_k	kth (k=0,1,2,...) moment of live (P_n) polymer radicals $\equiv \sum_{n=1}^{\infty} n^k P_n$, mol
μ_k	kth (k=0,1,2,...) moment of dead (D_n) polymer chains $\equiv \sum_{n=1}^{\infty} n^k D_n$, mol
μ_n	number average chain length at time t $\equiv(\lambda_1 + \mu_1)/(\lambda_o + \mu_o)$
μ_w	weight average chain length at time t

	$\equiv (\lambda_2 + \mu_2)/(\lambda_1 + \mu_1)$
ξ_{13}, ξ_{23}, ξ_{I3}	ratio of the molar volume of the monomer, solvent, and initiator jumping units to the critical molar volume of the polymer, respectively
ρ_m, ρ_p, ρ_s	density of pure (liquid) monomer, polymer or solvent at temperature T (at time t), kg m^{-3}
ϕ_m, ϕ_p, ϕ_s	volume fractions of monomer, polymer or solvent in liquid at time t
ψ, ψ_{ref}	defined in Eqs. 20 and 21 in Appendix I

Subscripts/Superscripts

exp	experimental value
Min	minimize
o	initial value
th	theoretical value

CHAPTER 1

INTRODUCTION

In free-radical polymerizations, the termination, propagation and initiation reactions (see Table 1) become diffusion-controlled as the conversion of monomer increases and the viscosity of the reaction mass goes up. The manifestations of these diffusion-controlled reactions (sharp and large increases in monomer conversion, x_m, with time after a certain period, increase in the weight average chain length, μ_w; see Nomenclature for symbols and definitions) are commonly referred to as the gel (or Trommsdorff),[1,2] glass and cage effects, respectively. A good model is required to account for these effects mathematically, so that it can be used for design, optimization and control purposes. A sample polymerization system exhibiting these phenomena is that of polymethyl methacrylate (PMMA), an important commodity plastic.

A vast amount of research has been reported in the open literature in the last two decades on the development of theoretical models for MMA polymerization. Chiu et al.[3] have developed a model having a molecular basis and used the Fujita-Doolittle free volume theory to account for the diffusional limitations of the termination and propagation rate constants, k_t and k_p. In this model, a set of algebraic equations were written for the gel and glass effects, using the initial number average chain length, $\mu_{n,o}$, as a parameter. Later, Achilias and Kiparissides[4,5] developed a model using the free

TABLE 1

KINETIC SCHEME FOR POLYMERIZATION OF MMA

(BULK AND SOLUTION POLYMERIZATIONS)

1. Initiation

$$I \xrightarrow{k_d} 2R$$

$$R + M \xrightarrow{k_i} P_1$$

2. Propagation

$$P_n + M \xrightarrow{k_p} P_{n+1}$$

3. Termination

by combination $\quad P_n + P_m \xrightarrow{k_{tc}} D_{n+m}$

by disproportionation $\quad P_n + P_m \xrightarrow{k_{td}} D_n + D_m$

4. Chain transfer to monomer

$$P_n + M \xrightarrow{k_f} P_1 + D_n$$

5. Chain transfer to monomer via solvent

$$P_n + S \xrightarrow{k_s} S^{\cdot} + D_n$$

$$S^{\cdot} + M \xrightarrow{\text{fast}} S^{\cdot} + D_n$$

or

$$P_n + M \xrightarrow{k_s} D_n + P_1$$

volume theory of Vrentas and Duda[6] and accounted for the diffusional effects on k_t, k_p, as well as the initiator efficiency, f. This model used the initial concentration of the initiator, $[I]_o$, as a parameter. Normally, industrial reactors are operated under nonisothermal or semibatch conditions with addition and removal of components like initiator, solvent and monomer. The models of Chiu et al. and Achilias and Kiparissides cannot be applied to these situations since the value of $\mu_{n,o}$ or $[I]_o$ is not precisely defined for such cases. Ray et al.[7] developed a model which did not have such limitations. They assumed the initiator efficiency to be constant and obtained expressions for two parameters of the model, $\theta_t(T)$ and $\theta_p(T)$, by curve-fitting experimental data[8,9] taken in small ampoules under isothermal conditions. The predictions made by their model for idealized, nonisothermal conditions (step changes in temperature) as well as for idealized semibatch operating conditions (intermediate addition of a solution of initiator in monomer), were found to be in good agreement with experimental observations[10,11]. This confirmed the adequacy of the model for simulation of polymerizations under industrially relevant conditions of operation.

More recently, Seth and Gupta[12] modified the model of Ray et al.[7] and also considered the variation of the initiator efficiency, f, with time. Their model used three parameters, $\theta_t(T)$, $\theta_p(T)$ and $\theta_f(T)$, representing the gel, glass and cage effects, respectively. They again curve-fitted the experimental data[8,9] on MMA polymerization under isothermal conditions in small ampoules (both for bulk polymerization with AIBN

initiator[8] as well as for solution polymerization in benzene with benzoyl peroxide[9]). Predictions of their 'tuned' model were found to be in better agreement with experimental data[10,11] taken under idealized nonisothermal and semibatch conditions, than the model of Ray et al. The complete set of equations for this model and the values of several parameters and physical properties required, are given in Appendices I and II.

With an appropriate model available for free-radical polymerizations, one can now think of studying the *on-line* optimizing control of these processes. An important step in such studies is the measurement of the *state* of the system at different times, t. Densitometers and gel permeation chromatography have been used in some experimental control studies[13-15] of *solution* polymerizations for estimating monomer conversions, $x_m(t)$, and the number average chain lengths, $\mu_n(t)$ [or the weight average chain lengths, $\mu_w(t)$]. However, these experimental techniques cannot be used conveniently for *bulk* polymerizations, and inferential state estimation techniques have to be resorted to. Seth and Gupta[12] and Chakravarthy et al.[16] have suggested the use of experimental values of the viscosity, $\eta(t)$, of the reaction mass [along with the measured values of the temperature, T(t)] for such purposes. Recently, Embirucu et al.[17], have surveyed the open literature on advanced control strategies for polymerization reactors, and have found that very few studies have been reported on property estimation techniques for the control of *bulk* polymerizations. There is, thus, a definite need to explore whether model-based inferential state estimation using T(t) and $\eta(t)$ is, indeed, feasible. If so, it

could be used experimentally (in the future) for on-line optimizing control of bulk polymerization reactors. This study presents some theoretical work along these lines for the sample system, PMMA.

CHAPTER 2

FORMULATION

Model

The kinetic scheme for MMA polymerization is shown in Table 1. A set of ordinary differential equations (ODEs) representing the mass balances and moment equations for a semibatch reactor can easily be written. These are of the form

$$d\underset{\sim}{x} / dt = \underset{\sim}{F}(\underset{\sim}{x}) ; \qquad \underset{\sim}{x}(t=0) = \underset{\sim}{x}_o \tag{1}$$

where $\underset{\sim}{x}(t)$ is the state variable vector defined by

$$\underset{\sim}{x} = [\, I,\ M,\ R,\ S,\ \lambda_0\ \lambda_1,\ \lambda_2,\ \mu_0,\ \mu_1,\ \mu_2,\ \zeta_m,\ \zeta_{m1}\ ] \tag{2}$$

The k^{th} ($k = 0, 1, 2$) moment of the radical and dead macromolecular species, P_n and D_n respectively, are represented by λ_k and μ_k (see Nomenclature). The exact equations are shown in Appendix I. Eqs. 1-12 of this Appendix account for intermediate additions and removals of components like initiator, solvent and monomer through the terms R_{li}, R_{ls}, R_{lm}, R_{vs} and R_{vm}. The conversion of monomer is defined as

$$x_m = 1 - (M / \zeta_{m1}) \tag{3}$$

where ζ_{m1} is the net monomer added to the reactor since the beginning of the operation.

The variation of the rate constants, k_t ($\equiv k_{td}$ for PMMA, since $k_{tc} \cong 0$), k_p, as well as the initiator efficiency, f, are described by the algebraic Eqs. 13-27 in Appendix I[12]. It is

observed that k_t, k_p and f depend on the current values of T, μ_n, λ_o, V_1, etc., and not on the initial conditions as in the models of Chiu et al.[3] and Achilias and Kiparissides[4,5]. This is why the model of Seth and Gupta[12] can be applied easily to nonisothermal and semibatch operations of reactors. The values of several properties and parameters required to integrate the equations in Appendix I are given in Appendix II (for *bulk* polymerization of MMA using AIBN initiator). The three parameters, $\theta_t(T)$, $\theta_p(T)$ and $\theta_f(T)$, have been expressed[12] in terms of second order polynomials in 1/T as shown in Appendix II. The equations in Appendix I can be integrated (for a given set of initial conditions[12]) using the NAG library program, D02EJF (which uses Gear's technique[18]), to obtain histories of monomer conversion and the number and weight average chain lengths. The value of the parameter, TOL, required in this code was 10^{-7} (the results were insensitive to decreases in the value of TOL). The values of the coefficients, a_1-a_3, b_1-b_3 and c_1-c_3, in the model have been obtained earlier[12] by curve-fitting experimental data under isothermal conditions on bulk[8] and solution[9] polymerization at several temperatures. In the present work, the parameters, a_1-a_3, b_1-b_3 and c_1-c_3, were re-tuned using only the bulk polymerization data[8] since these were of interest. These parameters were found to be quite close to values obtained by Seth and Gupta[12], and the new values are given in Appendix II.

An equation relating the viscosity, η, of the reaction mass and the temperature, T, to the state of the system (monomer conversion, x_m, and weight average molecular weight, M_w) is required so that model-based inferential state estimation can be

done. Moritz[19] has suggested the the use of the Lyons-Tobolsky[20] equation. This equation is a one-term adaptation of the more general series expression relating the specific viscosity, $(\eta/\eta_{sol}) - 1$, to the product of the intrinsic viscosity, $[\eta]$, and the polymer concentration, C_{polym}. We modified the Lyons-Tobolsky equation slightly to incorporate a higher-order (quadratic) term as shown in Appendix I (Eq. 28). This was done to obtain better predictions for some preliminary experimental data on nonreacting PMMA-MMA solutions at 50°C and 70°C, taken on a Haake^P Rotovisco RV20 viscometer in our laboratory[21] (see Appendix III). Such an empirical modification also helped in suppressing the temperature variation of the parameter, b, in the adapted Lyons-Tobolsky equation. The parameter, k_H, in this equation, which is a function of temperature, was tuned using the (preliminary) viscosity data generated in our laboratory, and two coefficients, d_1 and d_2, relating k_H to T using a linear variation, were so obtained. The values of d_1 and d_2 are given in Appendix II. It must be emphasized that more experimental data on the viscosity of (nonreacting) PMMA-MMA solutions at several *additional* temperatures and concentrations must be taken before the values of d_1 and d_2 (given in Appendix II) can be used for experimental studies. However, since the main objective of the present study was to explore whether viscosity measurements can be successfully used for model-based, on-line inferential state estimation, the use of the order-of-magnitude estimates of d_1 and d_2 given in Appendix II (based on the results taken over a restricted range of experimental conditions), is appropriate.

Generation of 'Experimental' Data

In order to explore the idea of using measured values of T(t) and $\eta(t)$ for inferential state estimation of bulk PMMA reactors, one needs to have experimental viscosity data for a given T(t) for a polymerizing system. Since this is not yet available, (pseudo) 'experimental' data are generated using the model itself, and some noise is superposed on the 'smooth' model-predictions to simulate actual experimental data. One of the optimal temperature histories for bulk polymerization of MMA, as provided by Chakravarthy et al.[16] recently, is selected (desired value of μ_n = 1800, and of monomer conversion, x_m = 0.94, to be obtained in the minimum reaction time) for this work. This 'smooth' temperature history, $T_{sm}(t)$, is curve-fitted using a 17^{th} order Chebyshev series (using the NAG library program, E02ADF) so that it can be provided as an input to the reactor-simulation program. A noise is superposed on $T_{sm}(t)$, using a random number, [R(t)], generator to give what can be considered as the 'experimental' temperature history, $T_{exp}(t)$:

$$T_{exp}(t_i) = T_{sm}(t_i) + [4R(t_i) - 2] \qquad (4)$$

In Eq. 4, R(t) is a random number lying between 0 and 1, generated using the NAG subroutine G05CCF. The term, $4R(t_i) - 2$, is used so as to give the amplitude of the noise as $2^{o}C$. The 'experimental' data *points* are generated using Eq.4 with t_i = $i(\Delta t)$, where Δt is taken as 0.5 min. The viscosity of the reaction mass for bulk polymerization of MMA has then been generated using the initial value of the initiator concentration, $[I]_o$, as 15.48 mol/m^3, and using $T_{exp}(t_i)$ [with linear

interpolation used between consecutive points of $T_{exp}(t_i)$ in D02EJF]. It is observed that the model values of $\eta(t)$ so obtained are quite smooth and we must, therefore, add on a noise again so as to provide simulated 'experimental' viscosity data. The following equation is used for this purpose :

$$\eta_{exp}(t_i) = [0.5 + R(t_i)]\ \eta(t_i)\ ;\ t_i = i(\Delta t) \qquad (5)$$

Use of Eq. 5 leads to fluctuations in η_{exp} ranging from 0.5η to 1.5η, a fairly large range as compared to the possible errors and fluctuations in real experimental viscosity data.

The 'experimental' temperature and viscosity data so generated (by simulation) are shown in Figs. 1 and 2. These data are used for studying model-based inferential state estimation. The final values of x_m and μ_n using T(t) given by the solid curve in Fig. 1 are 0.9408 and 1748, respectively (these differ slightly from the values in Ref. 16 because our parameters are slightly different).

Inferential State Estimation

In a typical polymerization reactor in which on-line optimizing control is implemented, one would have available, at time $t = t_1$, a set of experimental values of temperature and viscosity, $T_{exp}\ [i(\Delta t)]$ and $\eta_{exp}\ [i(\Delta t)]$; $i = 0, 1, 2, \ldots, t_1/(\Delta t)$. A short time-horizon for curve-fitting, $t_1 - N_1(\Delta t) \leq t \leq t_1$, is selected and the experimental points lying (only) in this horizon are used to estimate the values of several of the parameters in the model. Sequential quadratic programming (SQP)[22,23] has been used in this work to obtain best-fit values

of four parameters, a_1, b_1, c_1 and d_1 (referred to as a_1 - d_1; while assuming all the remaining parameters to be the same as given in Appendix II — these being called *reference values* henceforth). The objective function used for the optimization is

$$\underset{a_1 - d_1}{\text{Min}}\ E \equiv \sum_{i=t_1/(\Delta t) - N_1}^{t_1/(\Delta t)} \left[\frac{\eta_{exp}(t_i) - \eta_{th}(t_i)}{\eta_{th}(t_i)} \right]^2 \qquad (6)$$

where η_{exp} is the experimental value of the viscosity, and η_{th} is the value predicted by the model corresponding to the values of a_1- d_1 used. In order to obtain the model values of the several state variables (see Eq. 2) and η_{th} for $t_1 - N_1(\Delta t) \le t \le t_1$ (as required in Eq. 6), the initial conditions are taken to be the *model* values at $t = t_1 - N_1(\Delta t)$ as computed in the previous iteration (and stored). Also, a constant temperature is assumed for the duration $t_1 - N_1(\Delta t) \le t \le t_1$, which is the average of the 'experimental' values of temperature during this period. The NAG subroutine, E04UPF using SQP, has been used for obtaining the best-fit values of a_1- d_1 (which minimize the sum of square error, E, in Eq. 6). Table 2 gives the values of the computational parameters used with this code. The SQP procedure also requires initial guesses and bounds for the parameters, a_1- d_1, for each value of t_1. The initial guesses supplied for the first iteration [$t_1 = N_1(\Delta t)$] are given in Table 2. For subsequent values of t_1, the optimal values of the parameters in the previous iteration are used as the initial guess. The bounds on the parameters are also listed in Table 2. The bounds on a_1 - c_1 have been chosen such that variations of about a decade (at any given temperature) are permitted in the values of θ_t, θ_p and

TABLE 2

INITIAL GUESSES AND BOUNDS FOR GENERATING THE SOLUTION IN THE FIRST CURVE-FIT HORIZON, AND PARAMETERS USED IN THE SQP CODE

Parameter	Initial Guess	Lower Bound	Upper Bound
a_1	1.2416×10^{2}	1.2346×10^{2}	1.2446×10^{2}
b_1	8.0673×10^{1}	8.0071×10^{1}	8.1071×10^{1}
c_1	2.0168×10^{2}	2.014×10^{2}	2.024×10^{2}
d_1	0.3118	0.309×10^{0}	0.315×10^{0}
a_2	1.0314×10^{5}	1.03018×10^{5}	1.0334×10^{5}
b_2	7.5×10^{4}	7.4845×10^{4}	7.5168×10^{4}
c_2	1.445×10^{5}	1.4524×10^{5}	1.4556×10^{5}
d_2	9.93×10^{-4}	9.0×10^{-4}	1.0×10^{-3}
a_3	2.2735×10^{7}	2.2669×10^{7}	2.27743×10^{7}
b_3	1.765×10^{7}	2.75955×10^{7}	1.76999×10^{7}
c_3	2.7×10^{7}	2.6979×10^{7}	2.7083×10^{7}

Parameters in SQP Code[23]

Parameter	Value
tol_{ob}	10^{-3}
tol_{nl}	10^{-6}
$func_{pr}$	10^{-10}
tol_{act}	10^{-8}

θ_f (note that a_1- c_1 are independent of temperature). The bounds on d_1 are chosen so as to permit a fairly large variation in the viscosity of the reaction mass. Much smaller bounds would normally be used in experimental on-line control work.

In addition to obtaining best-fit values of a_1 - d_1 in any iteration of curve-fitting (each such iteration requiring several iterations in the SQP code for convergence to be attained), we have used the reactor simulation code to *predict* values of the state variables and of $\eta_{th}(t)$ for 'future' times, $t_1 \leq t \leq t_1 + N_2(\Delta t)$ [using $T_{expt}(t)$ in this prediction horizon]. These theoretical predictions could be compared to the 'experimental' data points of viscosity (in the prediction horizon) to find out how good is the (short-term) predictive capability of the model-based state estimation technique described herein. The computer code starts from t = 0 and uses the first N_1 points (first curve-fitting horizon) for curve-fitting (followed by prediction of N_2 points in the future). This completes the first iteration of curve-fitting. The experimental values of viscosity for $0 + N_3(\Delta t) \leq t \leq (N_1 + N_3)(\Delta t)$ are then used for the second iteration (second curve-fitting horizon). This continues till the end of polymerization. The values of N_3 can be selected so as to have some overlap between the successive curve-fitting horizons.

A few checks were made on the computer code to ensure that it is free of errors. When the optimization program was run using *all* the 'experimental' points (with no fluctuations introduced) and initial guesses were provided which differed from the reference values (Appendix II) of a_1- d_1, the

optimization code converged to the reference values. Some other checks were also conducted and led to the conclusion that the code was relatively free of errors. The CPU time taken for the optimization problem was about 30 s on a super-mini HP 9000/735 mainframe computer.

CHAPTER 3

RESULTS AND DISCUSSION

The optimization program was run on the 'experimental' data of viscosity and temperature (Figs. 1 and 2), using the following parameters (called reference values again)

$$N_1 = 5$$
$$N_2 = 5$$
$$N_3 = 1$$
$$\Delta t = 0.5 \text{ min} \qquad (7)$$

Thus, five 'data' points at a time are taken for curve-fitting, and the curve-fitting horizon shifts by one 'experimental' point at a time in this reference run (with four points common between consecutive curve-fitting horizons).

Fig. 3 shows the piece-wise fitted curve of $\eta(t)$ alongwith the 'experimental' data points. The solid curve in Fig. 3 consists of segments which extend for one Δt period (the non-overlapping domain between two consecutive curve-fitting horizons). The fit of the viscosity 'data' is seen to be quite good. Fig. 4 shows the variations of the parameters, a_1 - d_1, from horizon to horizon (the end-values of t of the curve-fitting horizons are shown in Fig. 4 on the abscissa). It is observed that there is a considerable amount of 'ringing' in the values of these parameters between the lower and upper bounds. It is demonstrated *later* in this paper that this is because we are trying to curve-fit only a small number (5) of experimental data

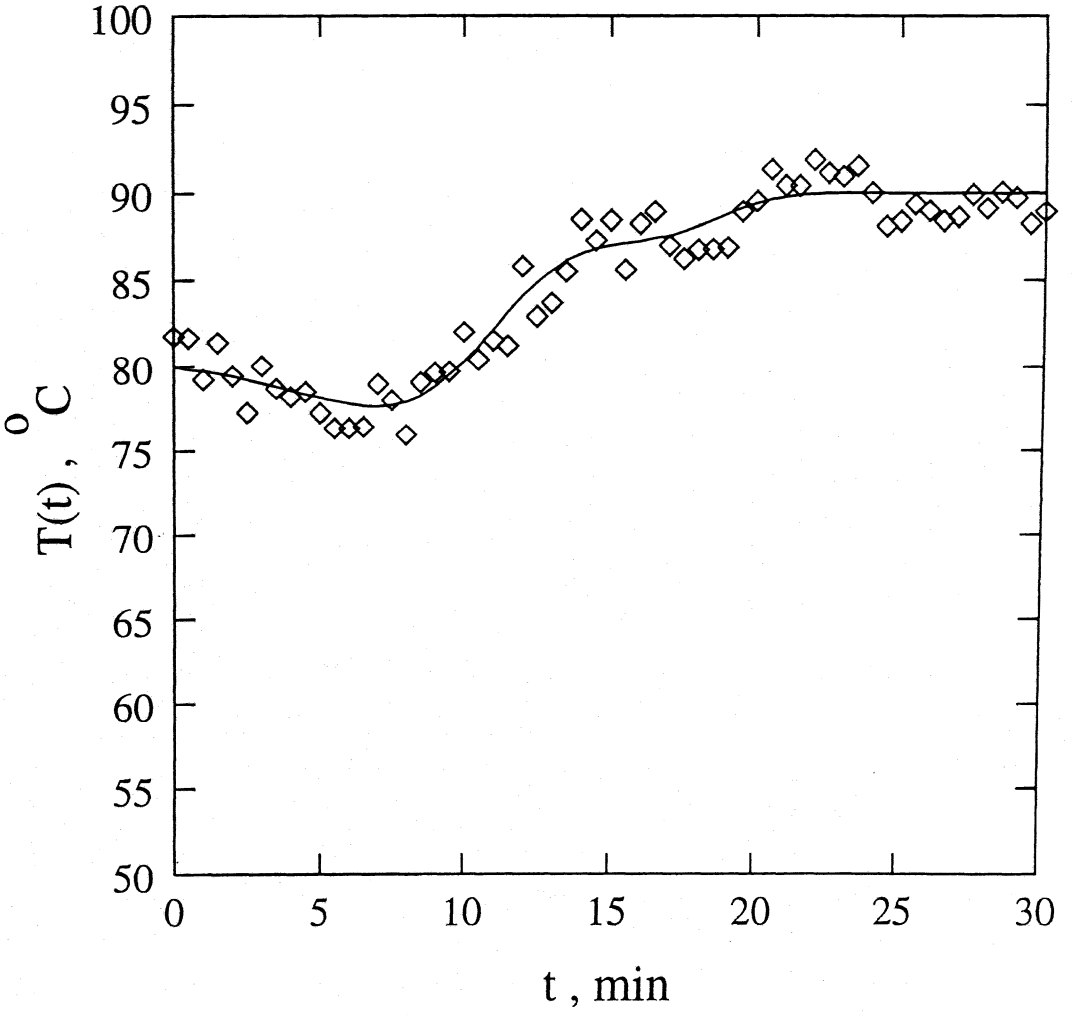

Fig. 1 : Continuous temperature history (solid curve) for $[I]_o$ = 15.48 mol/m^3 and randomized temperature 'data' points used in this study.

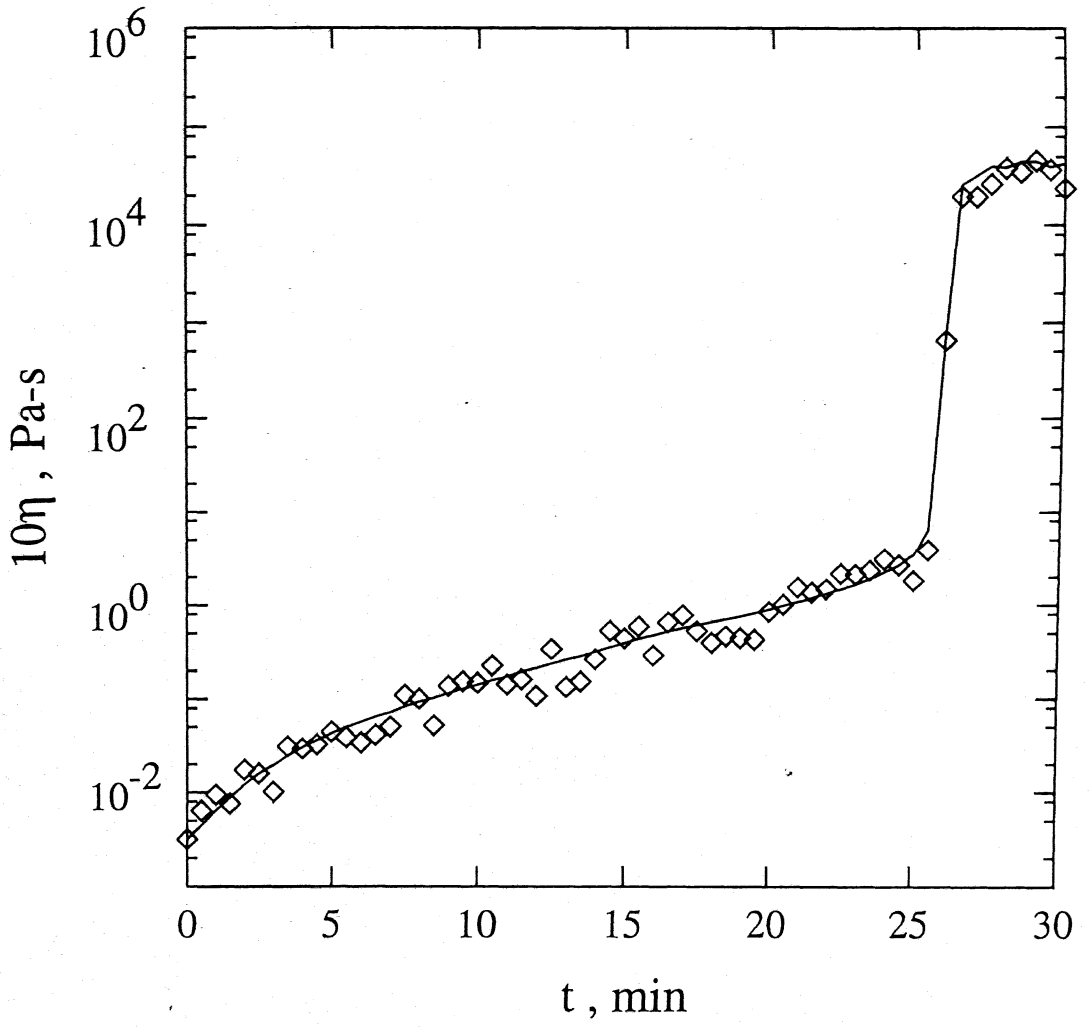

Fig. 2 : Viscosity (solid curve) of the reaction mass as generated using the temperature 'data' points of Fig. 1 with the model and best-fit values of the parameters as given in Appendix II. 'Experimental' viscosity data (points) obtained on randomization, also shown.

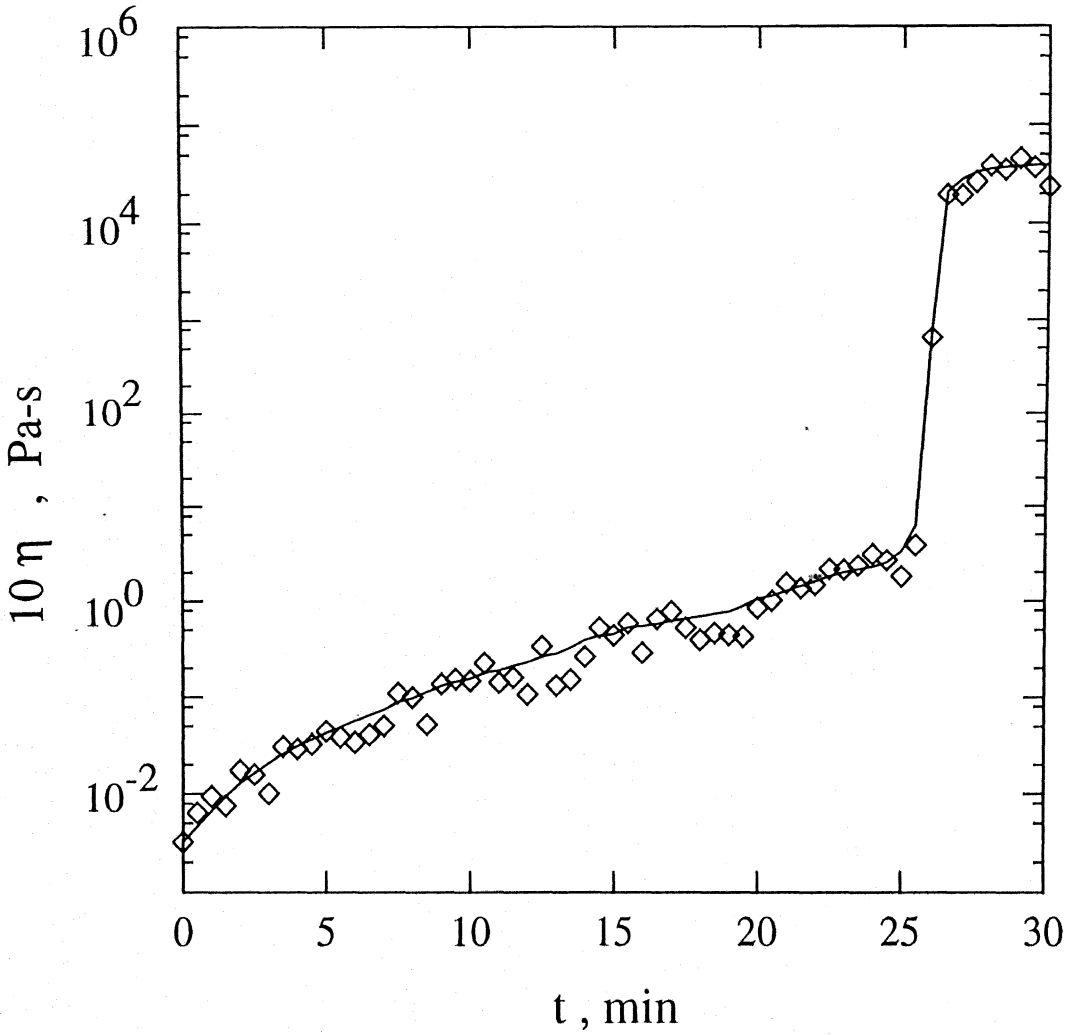

Fig. 3 : The curve-fitted viscosity (solid curve) for the reference case. 'Experimental' viscosity data, shown by

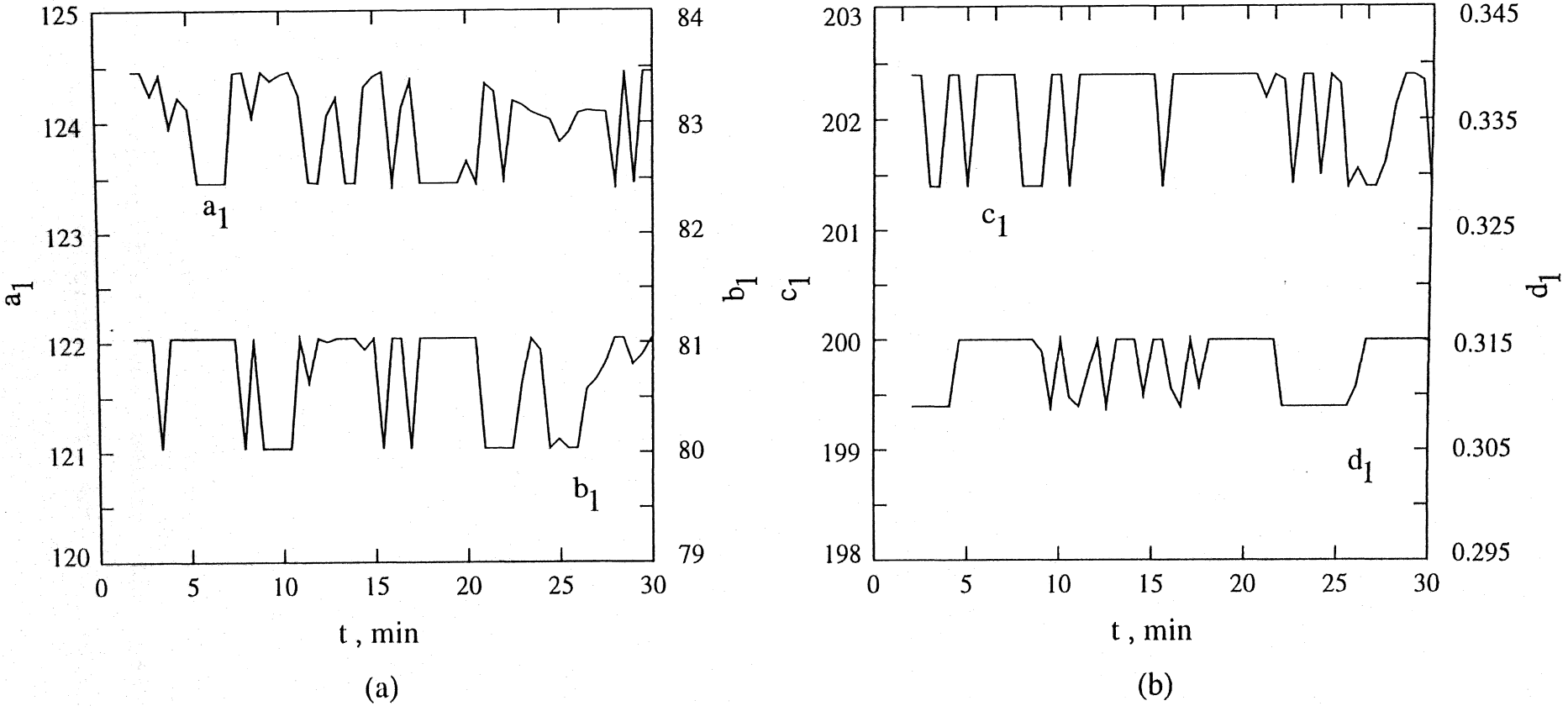

Fig. 4 : Variation of the parameters, a_1 - d_1, for the reference case, corresponding to the curve-fit of Fig. 3.

points in any one iteration, and that the ringing can be reduced by changing the bounds of the four parameters, as well as by increasing Δt. The corresponding variations in $\theta_t(T)$, $\theta_p(T)$, $\theta_f(T)$ and k_H are shown in Fig. 5. The ringing in the values of a_1 - d_1 are reflected as similar sharp fluctuations in the values of θ_t, θ_p, θ_f and k_H. In addition, there is a general change in these parameters associated with their temperature dependence[12]. The monomer conversion, M_n and M_w for the reference case are shown in Figs. 6 and 7. It is observed that the model predictions agree quite well with the 'experimental' points corresponding to the temperature 'data' of Fig. 1 (it may be noted that the viscosity 'data' were generated by introducing additional fluctuations to values computed using the 'data' of Figs. 6 and 7). The final values (at t = 30 min) of x_m and μ_n are found to be 0.9307 and 1743 respectively, for the curve-fitted case, as compared to the values of 0.9408 and 1748 corresponding to the temperature history shown by the solid (smooth) curve in Fig. 1. The small disagreements in these values are because of fluctuations introduced in T(t) and $\eta(t)$.

The optimal parameters obtained in any curve-fitting horizon are used with the temperatures in the corresponding prediction-horizon (five further points, since N_2 = 5) to predict the viscosity. The short-term prediction capabilities are shown in Fig. 8. It is clear from this figure that if the curve-fitting horizon is far ahead of the gel-effect, the short-term (N_2 = 5) predictions are quite good. When the curve-fitting horizon lies just before the gel-effect, the short-term future predictions need not be excellent. The

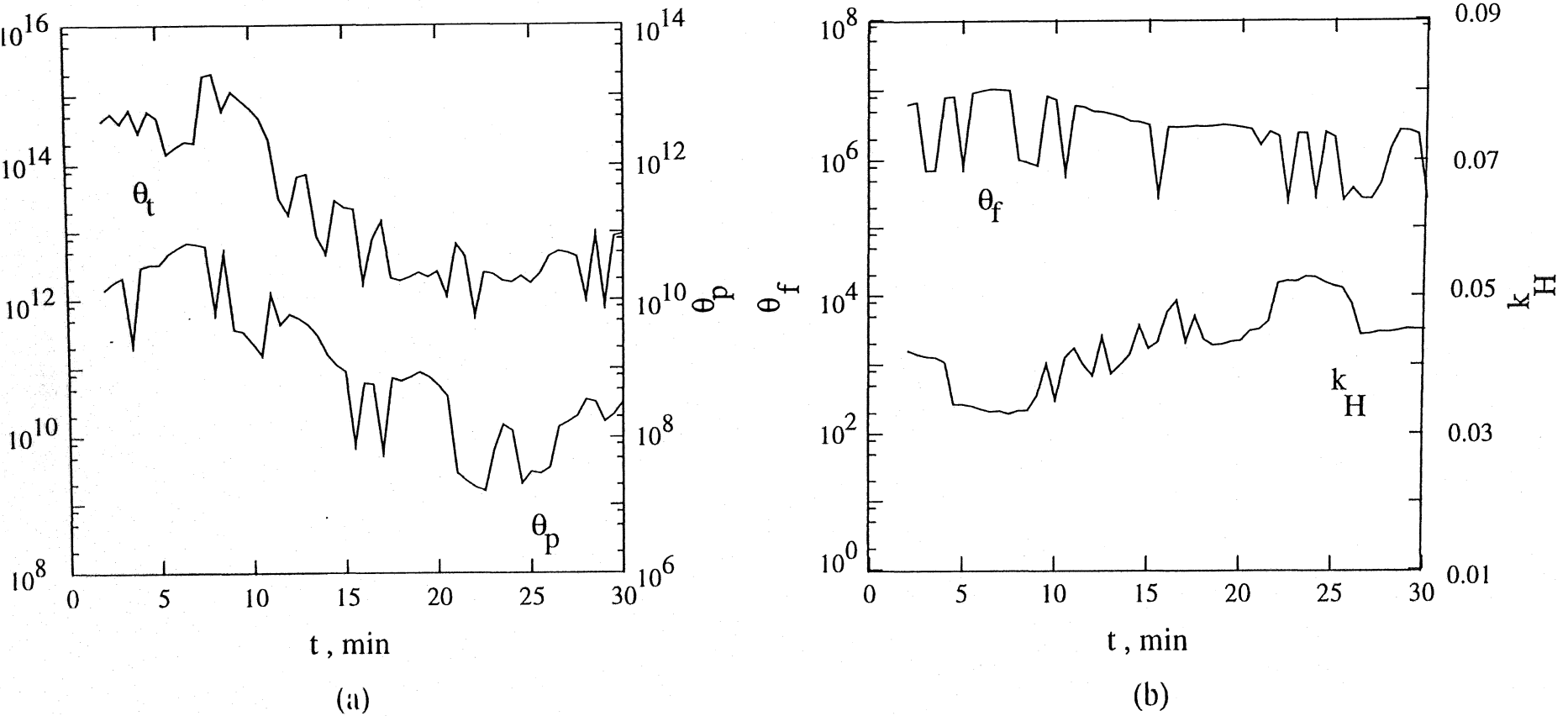

Fig. 5 : Variation of the parameters, $\theta_t(T)$, $\theta_p(T)$, $\theta_f(T)$ and $k_H(T)$, corresponding to the curve-fit of Fig. 3 (reference case).

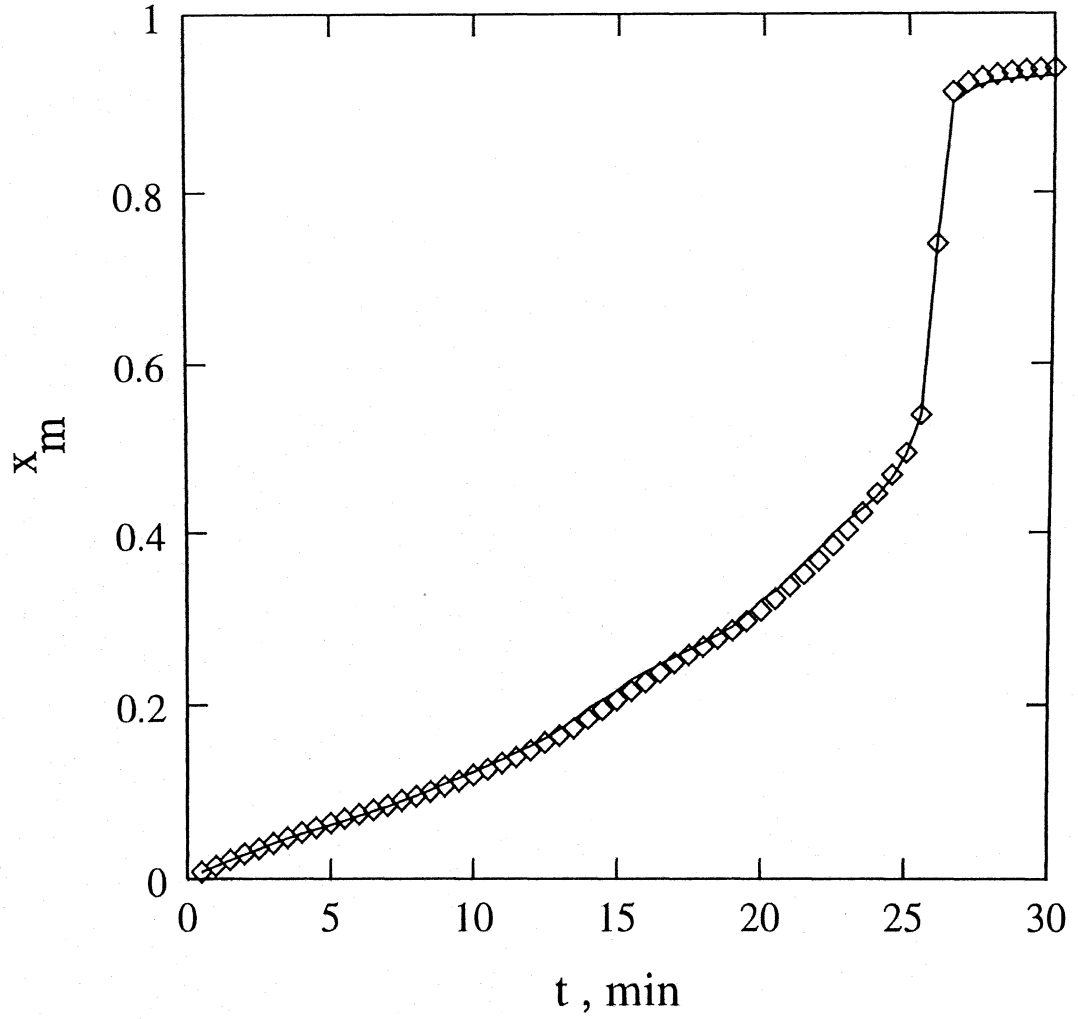

Fig. 6 : Estimated values of the monomer conversion (solid curve) for the reference case along with the 'experimental' data.

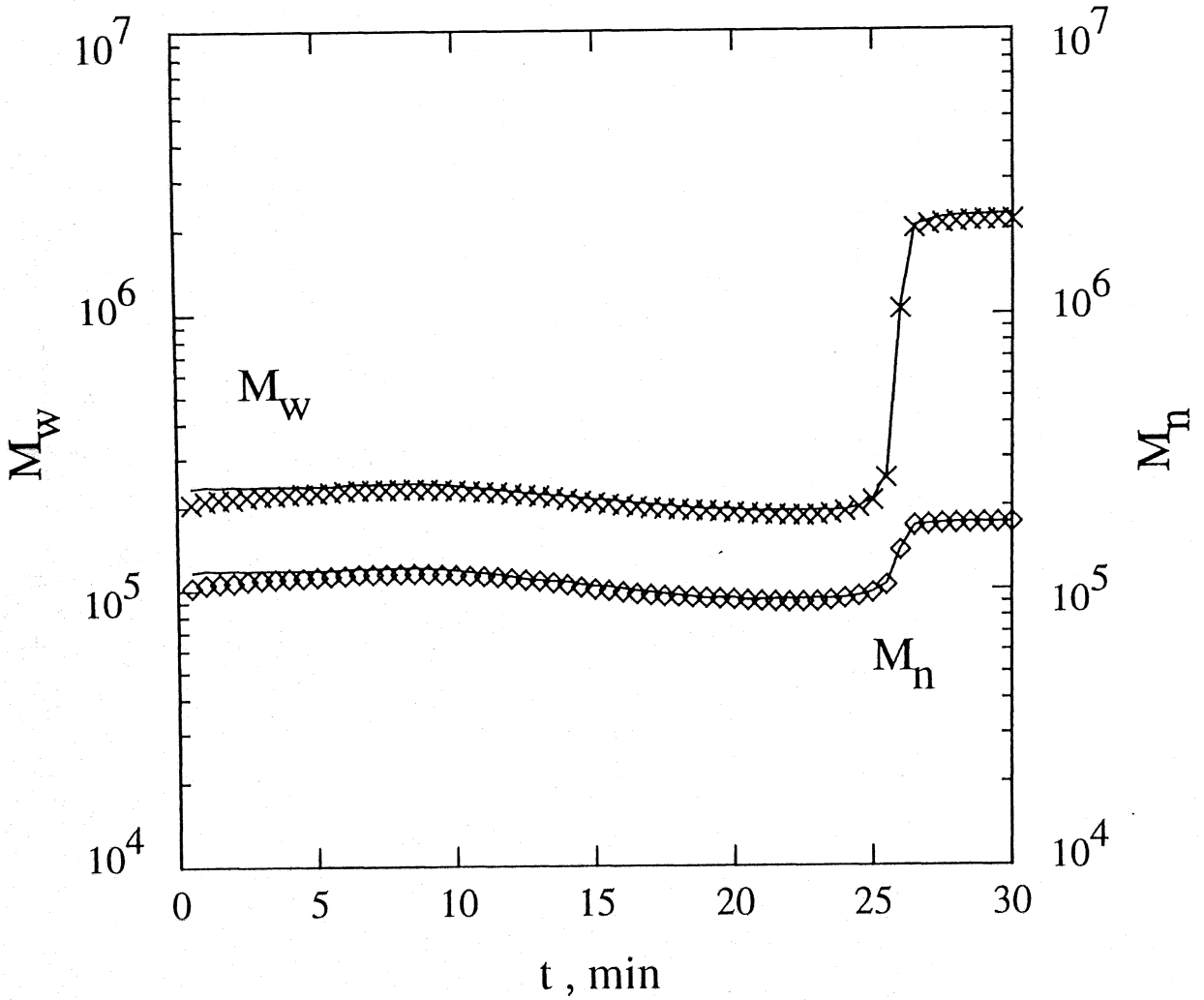

Fig. 7 : Estimated values of M_n and M_w (solid curve) for the reference case. 'Experimental' data on M_n and M_w obtained using the temperature 'data' of Fig. 1 with the best-fit values of the parameters (Appendix II) in

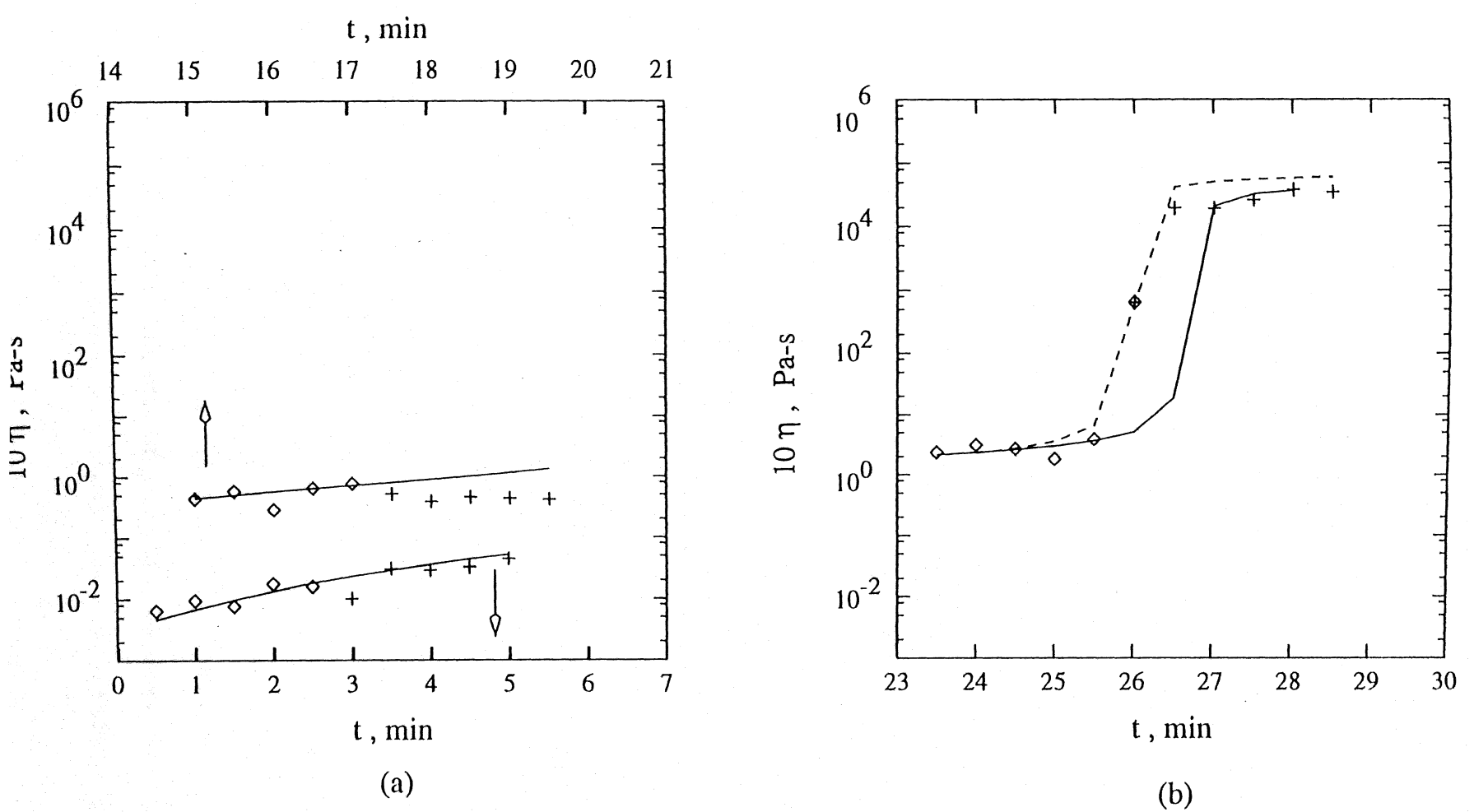

Fig. 8 : Short-range predictions for four curve-fitting horizons (reference case). Diamonds indicate the 'data' on η used for curve-fitting, while plusses indicate the 'data' in the prediction horizon. In Fig. 8b, the solid curve uses the first five points (starting from t = 23.5 min) for curve-fitting, while the dotted curve uses the five data points starting from t = 24 min.

predictions, however, improve considerably when *even a single data point* from the gel-effect region is included in the curve-fitting horizon. This is shown in Fig. 8b. Similar results are obtained for short-term predictions of x_m, μ_n and μ_w. All these reference results indicate that 'experimental' data on T(t) and $\eta(t)$ can indeed be used with a model to estimate the state variables of the system, e.g., $x_m(t)$, $\mu_n(t)$, $\mu_w(t)$ and $\eta(t)$.

It may be added that long-term predictions using the present technique may not be as good. For example, use of five 'experimental' points of $\eta(t)$ for curve-fitting the values of a_1 - d_1, and their subsequent use in the model with T(t); $t \geq t_1$, did not lead to as good an agreement of the predicted $\eta(t)$ with 'experimental' values in the gel-effect region (see Figs.9a and 10a). However, use of another set of five points leads to reasonable long-term predictions as shown in Figs. 9b and 10b (this is a consequence of the ringing in the values of the parameters). This *may* pose some problems in the use of this technique for on-line optimizing control purposes with minimization of the reaction time as the objective function. We feel, however, that multiple use of this technique (with shifting curve-fitting and prediction horizons) *may* overcome this problem, and the computed optimal temperature history may be satisfactory. Work is in progress to see if, indeed, this conjecture is true.

Having established the applicability of the technique described herein for inferential state-variable estimation, we now study the effect of varying several of the other parameters involved. Instead of using the most recent optimal values of a_1

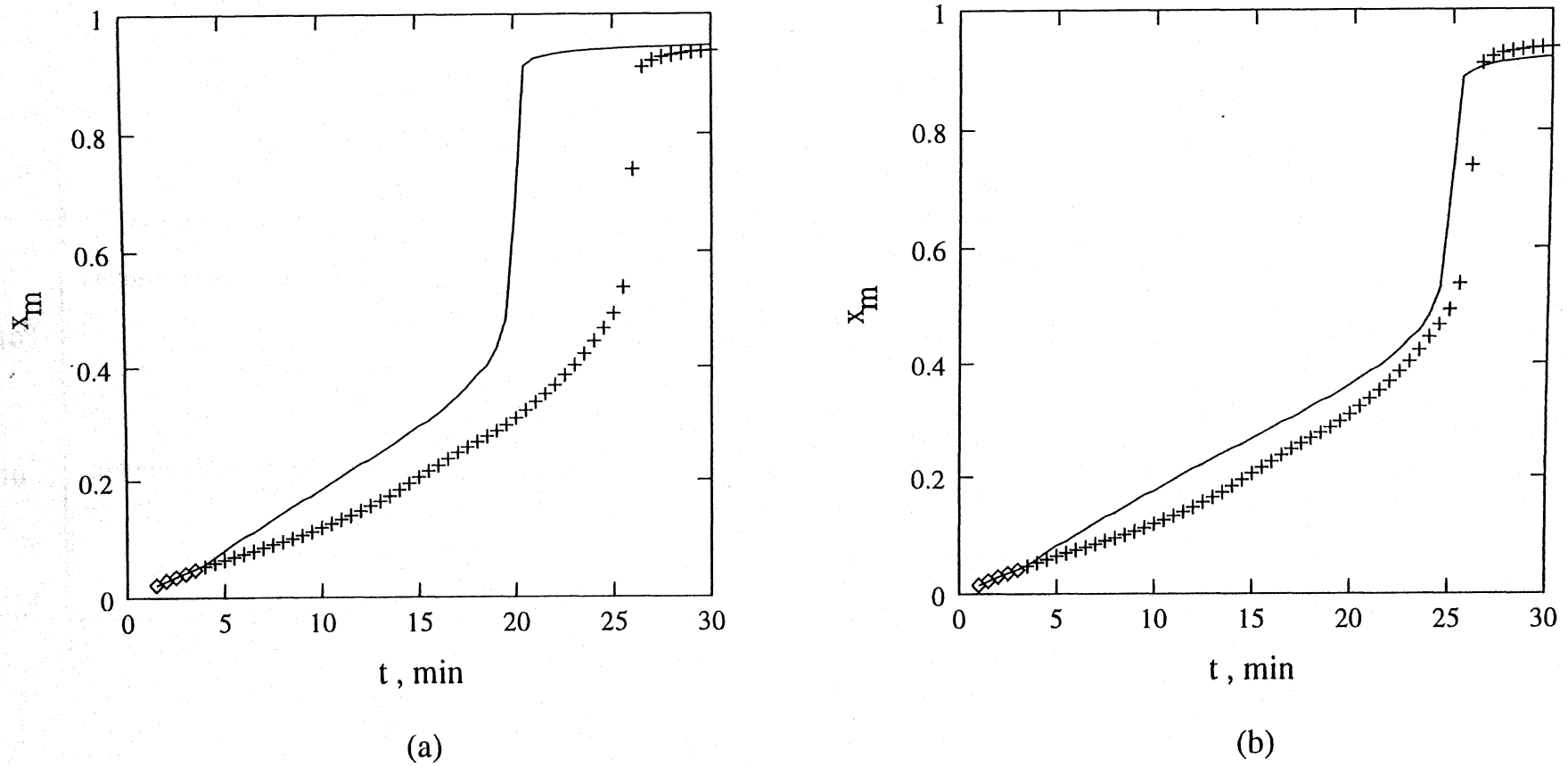

Fig. 9 : Long-range predictions for x_m (reference case) for two curve-fitting horizons. Notation same as in Fig. 8.

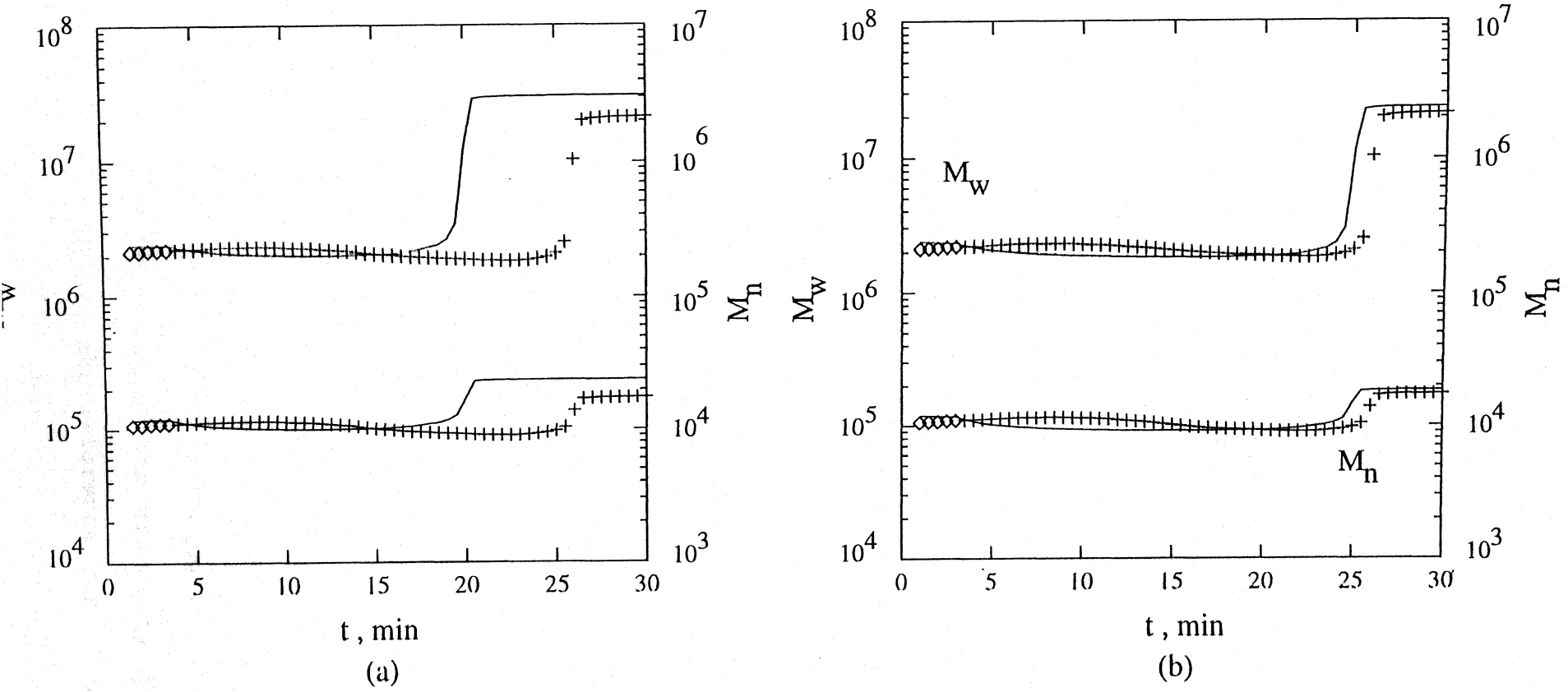

Fig. 10 : Long-range predictions for M_n and M_w (reference case) for two curve-fitting horizons. Notation same as in Fig. 8.

- d_1 as the initial guess values for any curve-fitting horizon, we used the initial values given in Table 2 for *all* the horizons. There was no perceptible change in the fit of the $\eta(t)$ data. Almost the same degree of ringing of the parameter values was observed. The CPU time was also about the same (increased by about 1s). These and other results not included in this paper for reasons of brevity, can be supplied on request.

In the reference run, we assumed a_2, a_3, b_2, b_3, c_2, c_3 and d_2 to be constants (at the values given in Table 2), and we obtained best-fit values of a_1, b_1, c_1 and d_1. We explored if there would be any improvement if all the 11 parameters (a_1 - d_2) were used for curve-fitting the $\eta(t)$ 'data'. The bounds of the remaining 7 parameters provided to the SQP code, as well as the initial guesses, are also given in Table 2. The bounds on a_2, a_3, b_2, b_3, and c_2, c_3 were selected so that each of them individually could give variations of about a decade in the values of θ_t, θ_p, and θ_f. The CPU time increased by about four fold, to 111 s. We observed that there was not much improvement in the fit of the viscosity data. Also, the degree of ringing in the 11 parameter, did not decrease much. Much larger oscillations were observed in the plots of $\theta_t(T)$, $\theta_p(T)$ and $\theta_f(T)$ for this case, possibly because of the adding-up of the effects of each of the additional parameters. Use of 11 parameters is, thus, not recommended since it provides no additional advantages over the use of 4 parameters (reference case).

We also studied the effect of narrowing the bounds on a_1 - d_1 by about 50%. The final fit of the viscosity data was about as good as that observed for the reference run (Fig. 3). But,

the ringing of the parameters, a_1 - d_1, reduced, as shown in Fig. 11. No worsening was observed in the short-term prediction capabilities. The final values of x_m, M_n and M_w were observed to be close to the reference values. The CPU time came down to 10 s. It can, thus, be inferred that narrowing the bounds for a_1 - d_1 is desirable for experimental, on-line optimizing control, and one needs to make a few test-runs to obtain the best-values.

We next studied the effect of increasing the value of N_1, the number of points used in the curve-fitting horizon, from 5 to 8. The fit of viscosity was observed to be as good as that shown in Fig. 3. The fluctuations in a_1 - d_1 reduced slightly as compared to the reference case, as shown in Fig. 12. The final values of x_m, M_n and M_w were in the desired range, as in the reference case. The prediction capabilities were also found to be about the same as for the reference case. The CPU time came down, as expected, to 15 s.

We, then, studied the effect of increasing the time interval, Δt, between 'data' points to 1 min (reference value = 0.5 min). The alternate 'data' points from the reference case (Figs. 1 and 2) were used for this purpose. The results obtained showed equally good fit of the viscosity data, as for the reference case. Fig. 13 shows that the degree of ringing in a_1 - d_1, with Δt = 1 min, is much less. The prediction capabilities and the final values of x_m, M_n and M_w, were found to be as good as for the reference case. The CPU time was 10 s. It is, thus, observed that larger values of Δt and narrower bounds on a_1 - d_1 than used for the reference case, are to be used for on-line optimizing control work. The best values of these can be

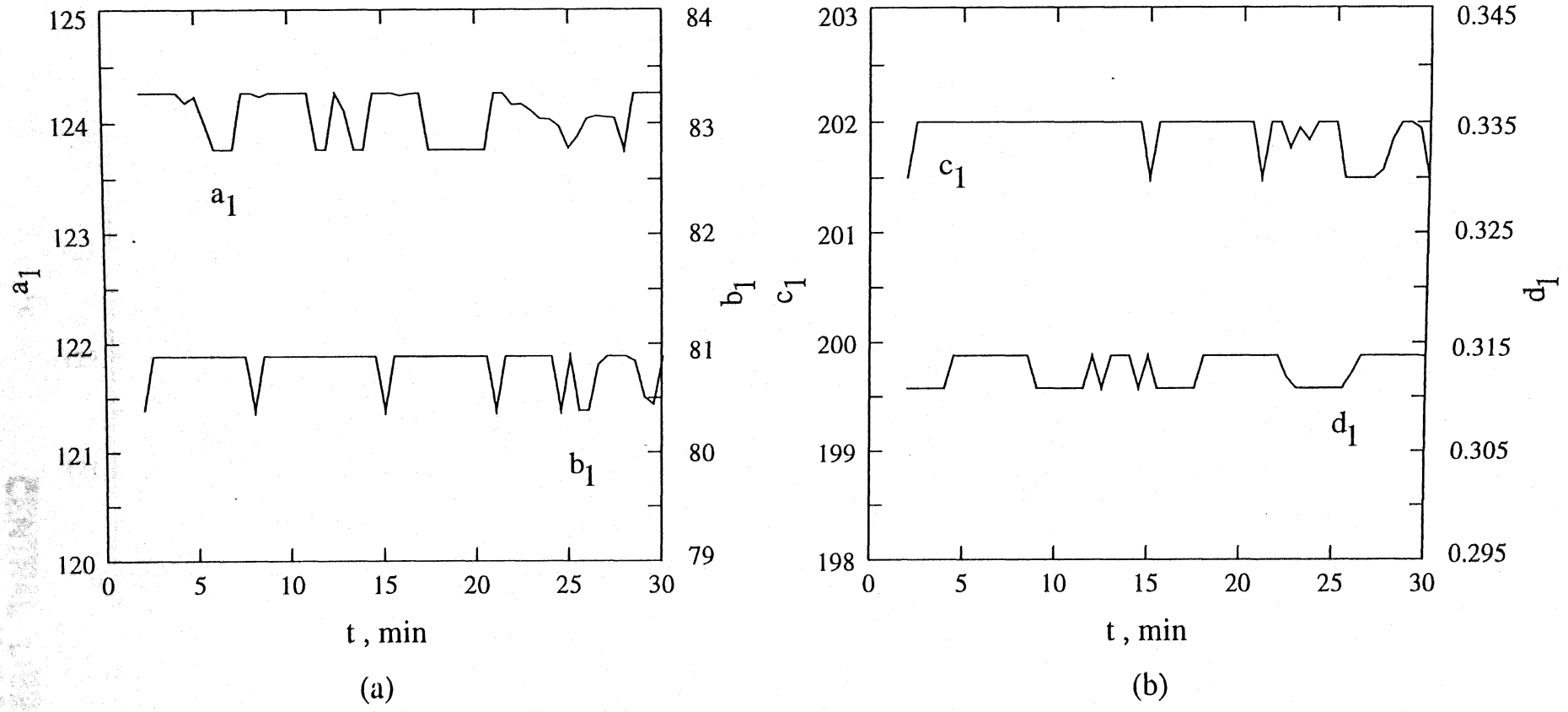

Fig. 11 : Variations of a_1 - d_1 for the case when their bounds (Table 2) are narrrowed down by 50 %.

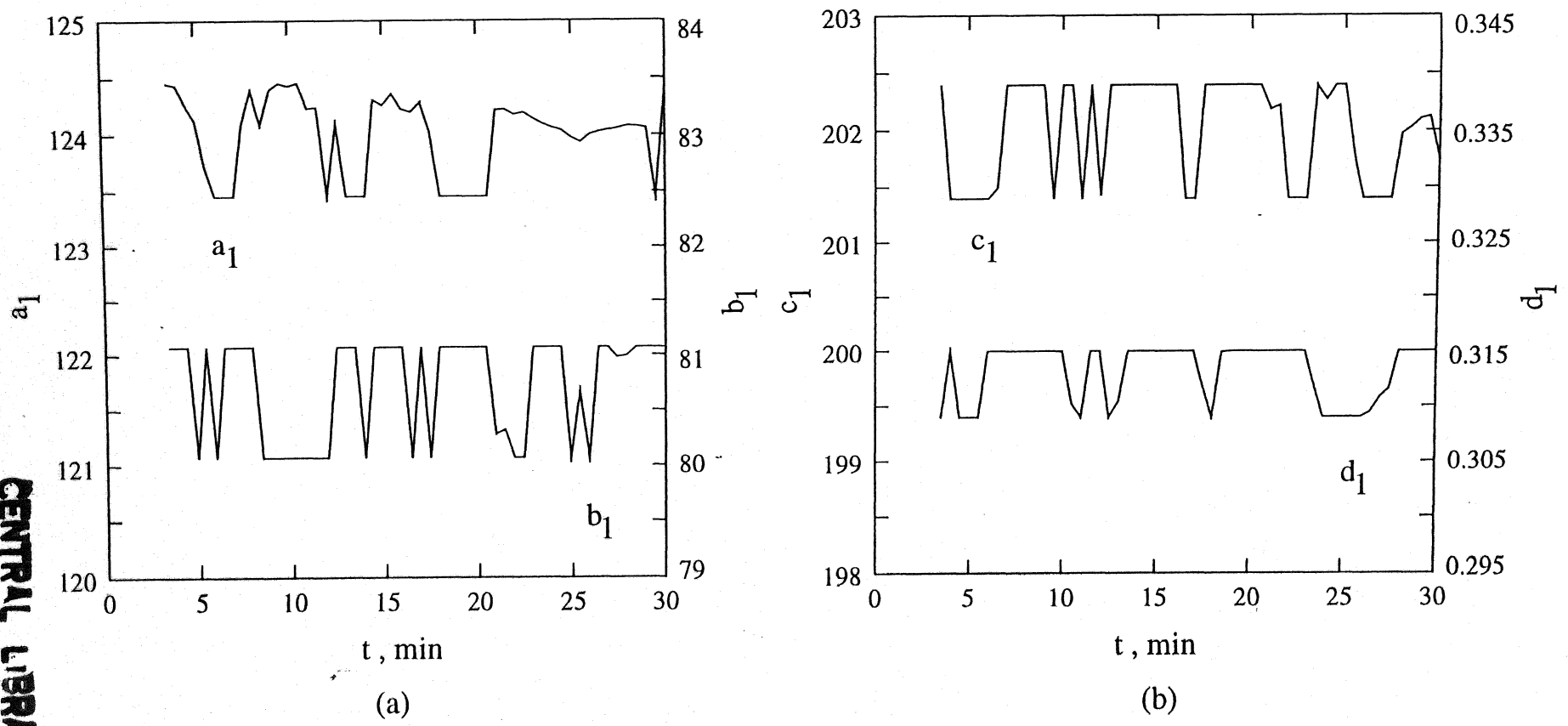

Fig. 12 : Variations of a_1 - d_1 when N_1 is increased from 5 to 8.

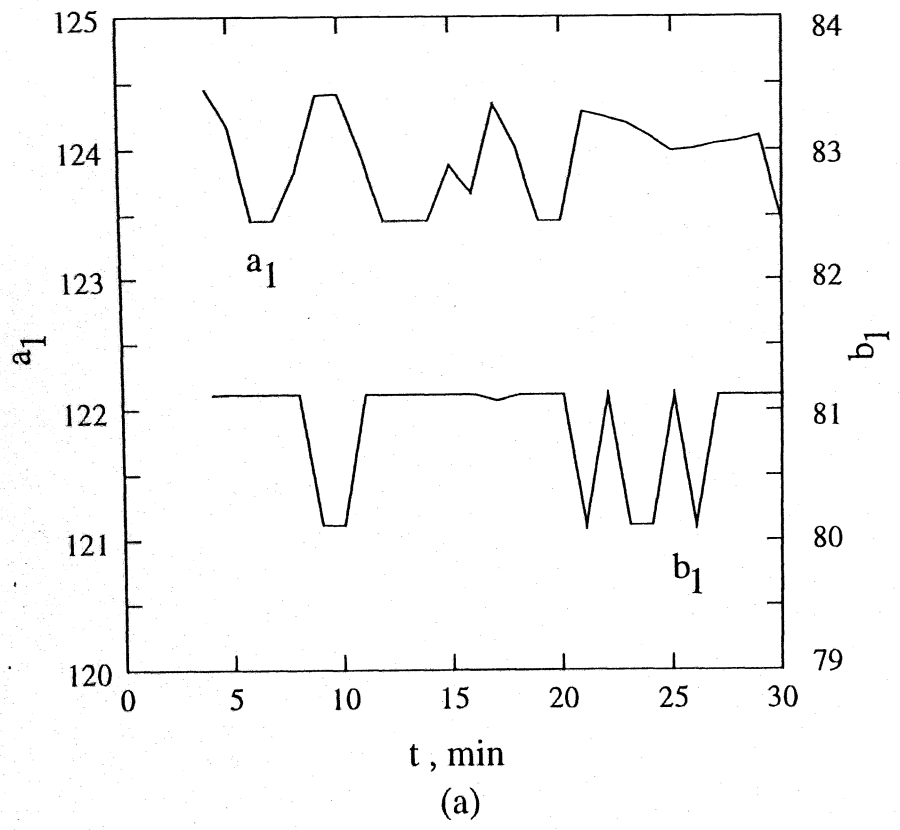

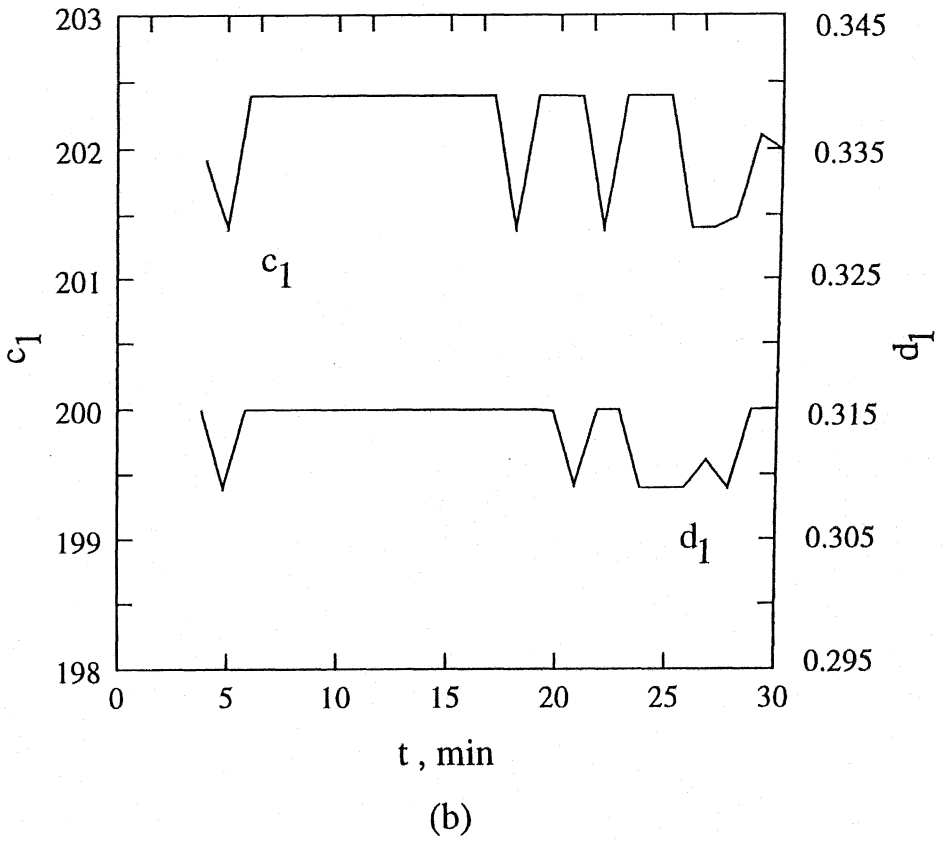

Fig. 13 : Variations of a_1 - d_1 when Δt is increased from 0.5 to 1 min.

obtained only after combining the present code with a program using genetic algorithm[16] to obtain optimal future temperature histories periodically.

We then explored the reasons for getting ringing in the values of the parameters. Isothermal (50°C) 'data' on $\eta(t)$, without any fluctuations introduced, was taken. This is shown in Fig. 14. The entire set of 66 points were curve-fitted to yield single values of the four parameters, a_1 - d_1, as shown bycurves *A* in Fig. 15. The same 'data' was curve-fitted using 35 data points each, with 4 overlapping points (see Table 3). Curves *B* in Fig. 15 show sudden and significant changes in the value of at least one parameter, c_1. Cases *C* - *D* in Fig. 15 show a significant amount of ringing as the number of curve-fitting horizons is increased. The fit of viscosity is equally good (as shown in Fig. 14 by the solid curve) in all the cases. It is, thus, clear that ringing is introduced by the use of only a few data points of viscosity, at a time, and that it is not caused by fluctuations in the data. The long-term predictions (for $N_1 = 5$), again, could be excellent or poor, because of the ringing in the values of the parameters.

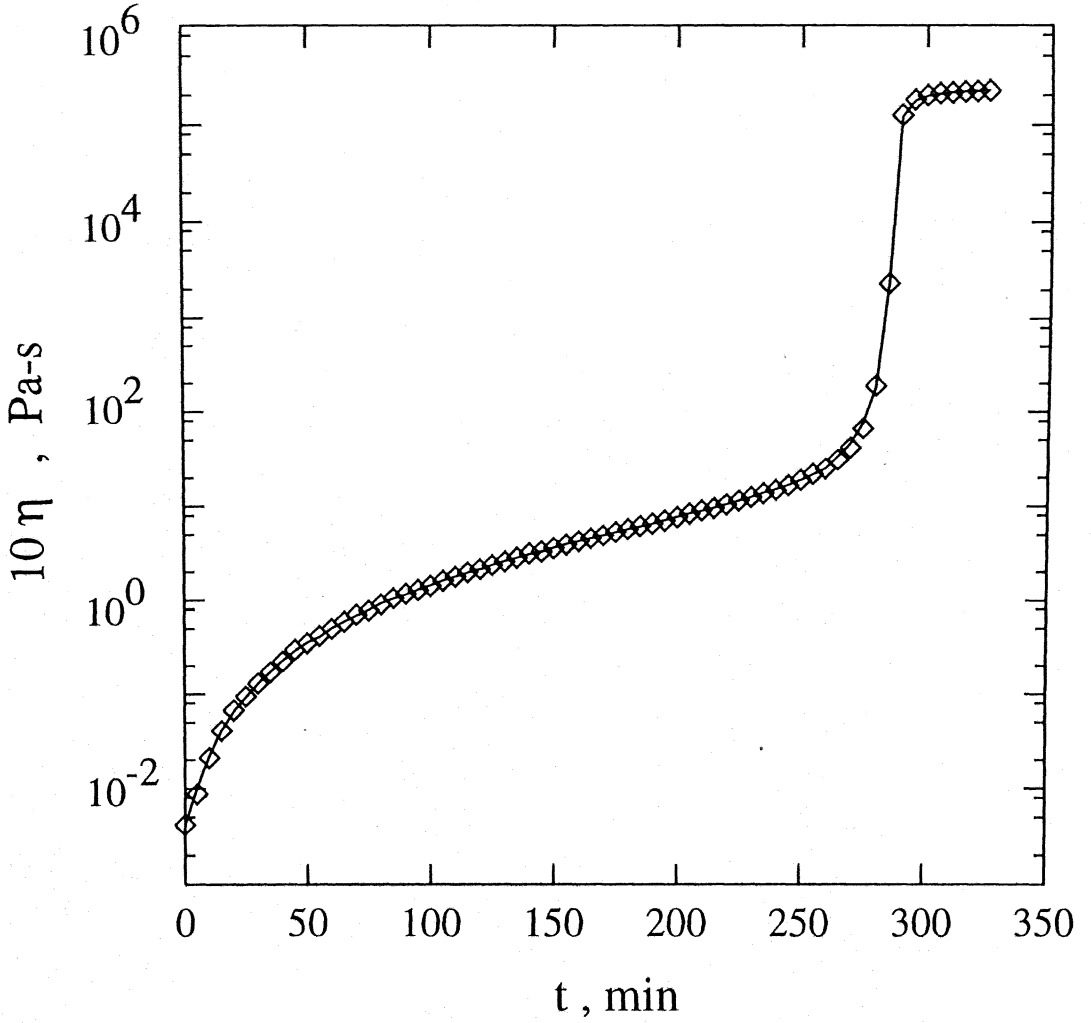

Fig. 14 : 'Experimental' viscosity data (points) under isothermal (50 ^{o}C) conditions with $[I]_o$ = 15.48 mol/m^3, in absence of any randomization. Solid curve is the curve-fitted one, with N_1 = 5 and N_3 = 10.

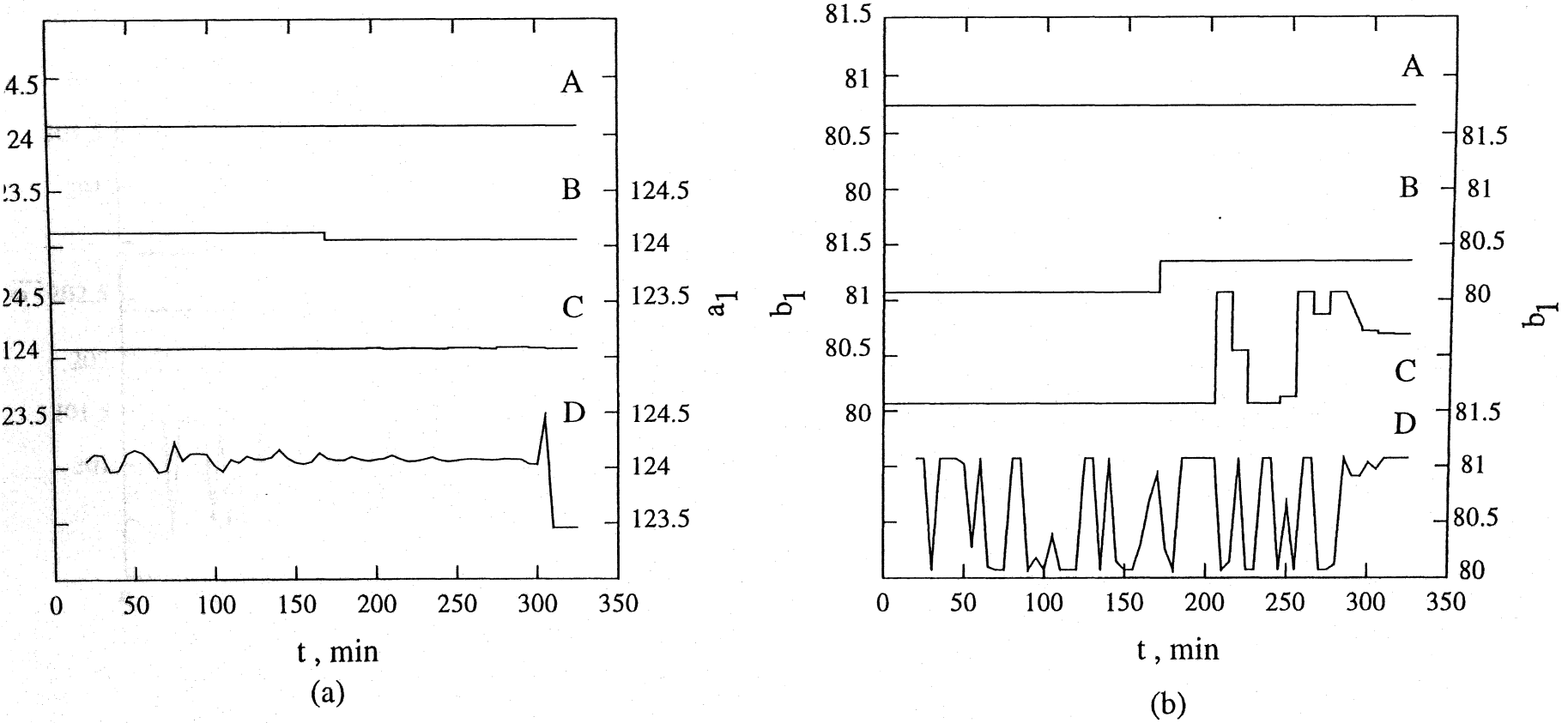

Fig. 15 : Variation of a_1 - d_1 for the curve-fitting of non-randomized, isothermal (50 ^{o}C) data shown in Fig. 14. Values of N_1 and N_3 for the various cases are given in Table 3. Scales for cases A and C are indicated on the left, while for cases B and D are on

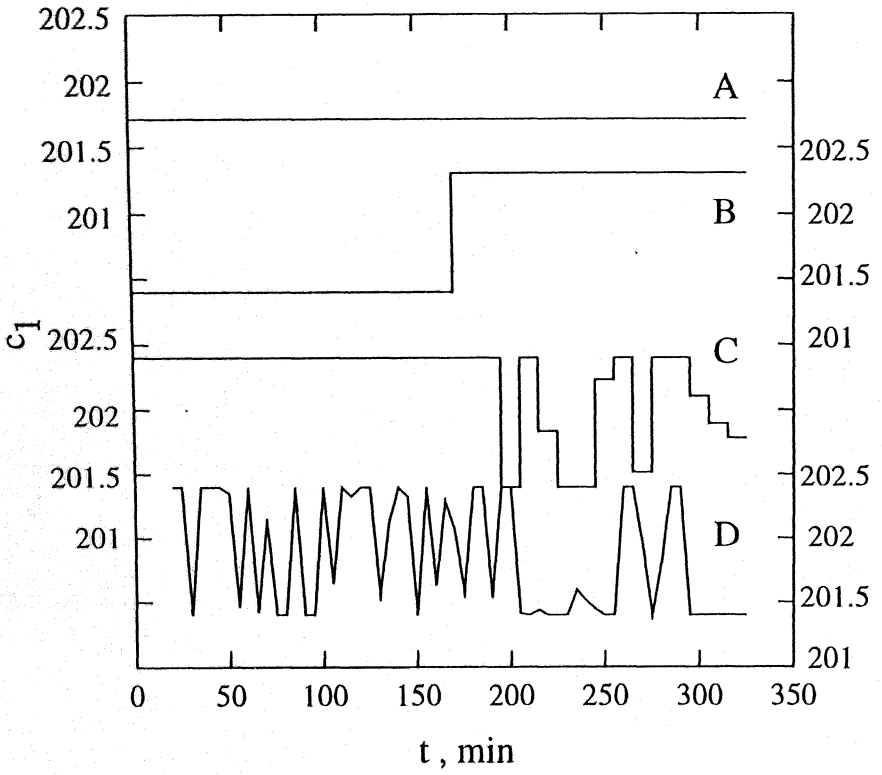
202.5
202
201.5
201
A
B
C
D
c_1
0
50
100
150
200
250
300
350
t , min

(c)

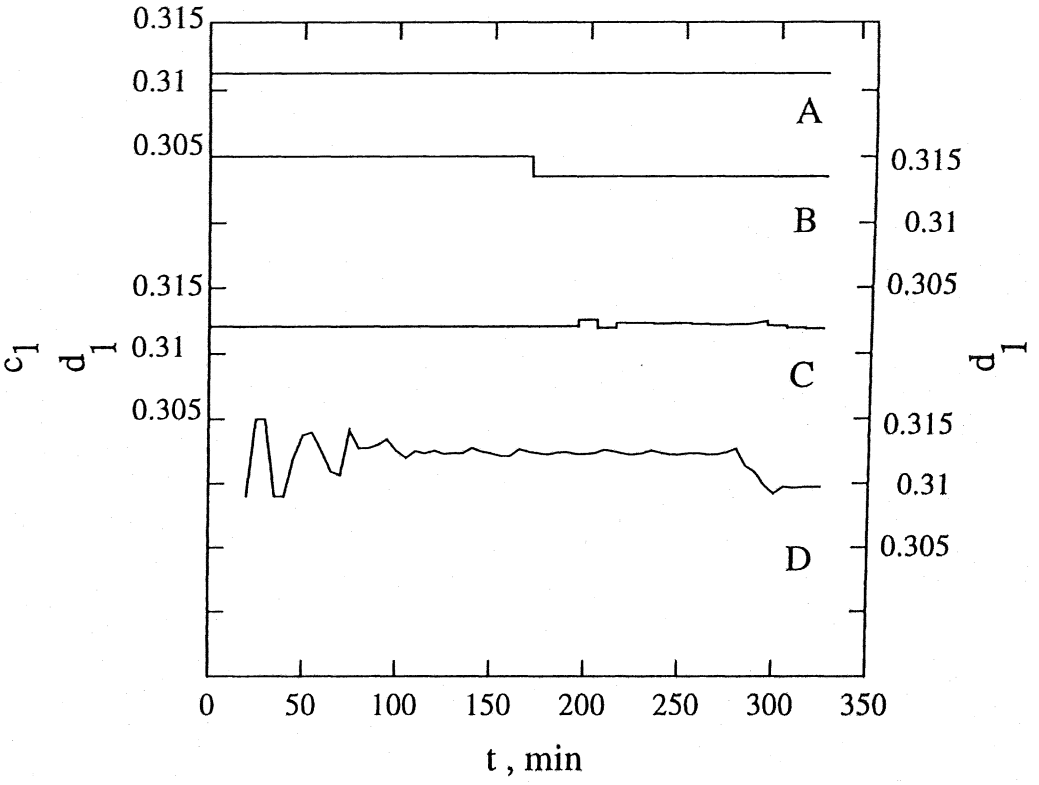
0.315
0.31
0.305
A
B
C
D
c_1
d_1
0
50
100
150
200
250
300
350
t , min

(d)

TABLE 3

DETAILS OF PARAMETERS USED FOR FITTING ISOTHERMAL VISCOSITY DATA OF FIG. 14 (Δt = 5 min)

Curve	N_1	N_3
A	66	-
B	35	01
C	40	02
D	05	01

CHAPTER 4

CONCLUSIONS

A model-based, inferential state-variable estimation technique has been described which uses a few of the most recent 'data' points on the viscosity of the reaction mass (moving curve-fitting horizon) to predict x_m, μ_n and μ_w. Short-term predictions in the moving prediction-horizon are found to be quite good, except when the curve-fitting horizon is very near to the get-effect region and does not include any data point in this region. Long-term predictions may or may not be excellent, depending on which curve-fitting horizon is used. Multiple curve-fitting followed by periodic determination of the optimal temperature history in the remaining period of polymerization could provide a satisfactory scheme for on-line optimizing control.

ACKNOWLEDGEMENT

This study was supported partially by a grant from the Department of Science and Technology, New Delhi.

CHAPTER 5

SUGGESTIONS FOR FUTURE WORK

Combining this work, periodic state-variable estimation, with the determination optimal temperature history in the future it could be seen whether this could be a feasible strategy for experimental on-line optimizing control of bulk free-radical polymerizations exhibiting Trommsdorff effect.

REFERENCES

1. R. G. W. Norrish and R. R. Smith, *Nature,* **150,** 336 (1942).
2. E. Trommsdorff, H. Kohle and P. Lagally, *Makromol. Chem.,* **1,** 169 (1947).
3. W. Y. Chiu, G. N. Carratt and D. S. Soong, *Macromolecules,* **16,** 348 (1983).
4. D. Achilias and C. Kiparissides, *J. Appl. Polym. Sci.,* **35,** 1303 (1988).
5. D. S. Achilias and C. Kiparissides, *Macromolecules,* **25,** 3739 (1992).
6. J. S. Vrentas and J. L. Duda, *AIChE J,* **25,** 1 (1979).
7. A. B. Ray, D. N. Saraf and S. K. Gupta, *Polym. Eng. Sci.,* **35,** 1290 (1995).
8. S. T. Balke and A. E. Hamielec, *J Appl. Polym. Sci.,* **17,** 905 (1973).
9. G. V. Schultz and G. Harborth, *Makromol. Chem.,* **1,** 106 (1947).
10. T. Srinivas, S. Sivakumar, S. K. Gupta and D. N. Saraf, *Polym. Eng. Sci.,* **36,** 311 (1996).
11. V. Dua, D. N. Saraf and S. K. Gupta, *Polym. Eng. Sci.,* **59,** 749 (1996).
12. V. Seth and S. K. Gupta, *J. Polym. Eng.,* **15,** 283 (1995).
13. M. Soroush and C. Kravaris, *AIChE J,* **38,** 1429 (1992).
14. M. F. Ellis, T. W. Taylor and K. F. Jensen, *AIChE J,* **40,** 445 (1994).
15. T.J. Crowley and K. Choi, *J. Process Control,* **6,** 119 (1996).
16. S. S. S. Chakravarthy, D. N. Saraf and S. K. Gupta, *J. Appl.*

Polym. sci., in press.

17. M. Embirucu, E. L. Lima and J. C. Pinto, *Polym. Eng. Sci.*, **36**, 433 (1996).

18. S.K. Gupta, *Numerical Methods for Engineers*, New Age Intl./ Wiley Eastern, New Delhi, 1995.

19. H.U. Moritz, *Chem. Eng. Technol.*, **12**, 71 (1989).

20. P. F. Lyons and A. V. Tobolsky, *Polym. Eng. Sci.*, **10**, 1 (1970).

21. R.B. Mankar, P. Ghosh, D.N. Saraf and S.K. Gupta, to be published.

22. P.E. Gill, W. Murray and M.H. Wright, *Practical Optimization*, Academic Press, New York, 1981.

23. R. Sareen and S.K. Gupta, *J. Appl. Polym. Sci.*, **58**, 2357 (1995).

APPENDIX I

MODEL EQUATIONS FOR MMA POLYMERIZATION IN SEMIBATCH REACTORS[12]

(BULK AND SOLUTION POLYMERIZATION*)

1. $$\frac{dI}{dt} = -k_d I + R_{1i}(t)$$

2. $$\frac{dM}{dt} = -(k_p + k_f)\frac{\lambda_o M}{V_1} - k_i \frac{R M}{V_1} - k_s S \frac{\lambda_o}{V_1} + R_{1m}(t) - R_{vm}(t)$$

3. $$\frac{dR}{dt} = 2fk_d I - k_i \frac{R M}{V_1}$$

4. $$\frac{dS}{dt} = R_{1s}(t) - R_{vs}(t)$$

5. $$\frac{d\lambda_o}{dt} = k_i \frac{R M}{V_1} - k_t \frac{\lambda_o^2}{V_1}$$

6. $$\frac{d\lambda_1}{dt} = k_i \frac{R M}{V_1} + k_p M \frac{\lambda_o}{V_1} - k_t \frac{\lambda_o \lambda_1}{V_1} + (k_s S + k_f M)\frac{(\lambda_o - \lambda_1)}{V_1}$$

7. $$\frac{d\lambda_2}{dt} = k_i \frac{R M}{V_1} + k_p M \frac{\lambda_o + 2\lambda_1}{V_1} - k_t \frac{\lambda_o \lambda_2}{V_1} + (k_s S + k_f M)\frac{(\lambda_o - \lambda_2)}{V_1}$$

8. $$\frac{d\mu_o}{dt} = (k_s S + k_f M)\frac{\lambda_o}{V_1} + (k_{td} + \frac{1}{2}k_{tc})\frac{\lambda_o^2}{V_1}$$

Contd...b

9. $$\frac{d\mu_1}{dt} = (k_s S + k_f M)\frac{\lambda_1}{V_l} + k_t \frac{\lambda_o \lambda_1}{V_l}$$

10. $$\frac{d\mu_2}{dt} = (k_s S + k_f M)\frac{\lambda_2}{V_l} + k_t \frac{\lambda_o \lambda_2}{V_l} + k_{tc}\frac{\lambda_1^2}{V_l}$$

11. $$\frac{d\xi_m}{dt} = R_{lm}(t) - R_{vm}(t)$$

12. $$\frac{d\xi_{m_1}}{dt} = R_{lm}(t)$$

13. $$V_l = \frac{S\ (MW_s)}{\rho_s} + \frac{M\ (MW_m)}{\rho_m} + \frac{(\xi_m - M)\ (MW_m)}{\rho_p}$$

14. $$\phi_m = \frac{M(MW_m)/\rho_m}{\frac{M(MW_m)}{\rho_m} + \frac{S(MW_s)}{\rho_s} + \frac{(\xi_m - M)(MW_m)}{\rho_p}}$$

15. $$\phi_s = \frac{S(MW_s)/\rho_s}{\frac{M(MW_m)}{\rho_m} + \frac{S(MW_s)}{\rho_s} + \frac{(\xi_m - M)(MW_m)}{\rho_p}}$$

16. $$\phi_p = 1 - \phi_m - \phi_s$$

17. $$\frac{1}{f} = \frac{1}{f_o}\left[1 + \theta_f(T)\ \frac{M}{V_l}\ \frac{1}{\exp\left[\xi_{I3}\left\{-\psi + \psi_{ref}\right\}\right]}\right]$$

Contd...c

18. $$\frac{1}{k_t} = \frac{1}{k_{t,o}} + \theta_t(T)\ \mu_n^2\ \frac{\lambda_o}{V_l}\ \frac{1}{\exp\left[\ -\psi + \psi_{ref}\ \right]}$$

19. $$\frac{1}{k_p} = \frac{1}{k_{p,o}} + \theta_p(T)\ \frac{\lambda_o}{V_l}\ \frac{1}{\exp\left[\ \xi_{13}\left\{-\psi + \psi_{ref}\right\}\ \right]}$$

20. $$\psi = \frac{\gamma\ \left\{\ \frac{\rho_m \phi_m\ \hat{V}_m^*}{\xi_{13}} + \frac{\rho_s\ \phi_s \hat{V}_s^*}{\xi_{23}} + \rho_p\ \phi_p \hat{V}_p^*\ \right\}}{\rho_m\ \phi_m\ \hat{V}_m^*\ V_{fm} + \rho_s\ \phi_s\ \hat{V}_s^*\ V_{fs} + \rho_p\ \phi_p\ \hat{V}_p^*\ V_{fp}}$$

21. $$\psi_{ref} = \frac{\gamma}{V_{fp}}$$

22. $$\xi_{13} = \frac{\hat{V}_m^*\ (MW_m)}{\hat{V}_p^*\ M_{jp}}$$

23. $$\xi_{23} = \frac{\hat{V}_s^*\ (MW_s)}{\hat{V}_p^*\ M_{jp}}$$

24. $$\xi_{I3} = \frac{\hat{V}_I^*\ (MW_I)}{\hat{V}_p^*\ M_{jp}}$$

25. $$k_d = k_d^o \exp\ (-E_d/RT)$$

26. $$k_{p,o} = k_{p,o}^o \exp\ (-E_p/RT)$$

27. $$k_{t,o} = k_{td,o} = k_{td,o}^o \exp\ (-E_{td}/RT)$$

Contd...d

Appendix I (contd....d)

28. $$\eta = \eta_{sol}\left[1 + C_{polym}\,[\eta]\,\exp\left(\frac{k_H\,[\eta]\,C_{polym}}{1 - b\,C_{polym}}\right) + C_{polym}^2\,[\eta]^2\,\exp\left(\frac{2k_H\,[\eta]\,C_{polym}}{1 - b\,C_{polym}}\right)\right]$$

29. $$C_{polym} = \rho_p\,\phi_p$$

30. $$[\eta] = K\,M_w^a$$

---

* no inert solvent (benzene) used in this work

Note: variables not defined in the Nomenclature are defined in Refs. 7 and 12.

APPENDIX II

PARAMETERS USED FOR BULK POLYMERIZATION OF MMA WITH AIBN[12]

ρ_m = 966.5 - 1.1 (T - 273.1) kg/m^3

ρ_p = 1200 kg/m^3

f_o = 0.58

k_d^o = 1.053x10^{15} s^{-1}

$k_{p,o}^o$ = 4.917x10^2 m^3/mol-s

$k_{td,o}^o$ = 9.8x10^4 m^3/mol-s

k_{tc} = 0.0

k_f = 0.0

k_i = k_p

k_s = 0.0

E_d = 128.45 kJ/mol

E_p = 18.22 kJ/mol

E_{td} = 2.937 kJ/mol

(MW_m) = 0.10013 kg/mol

(MW_I) = 0.06800 kg/mol

Parameters for the Cage, Gel and Glass Effects

$\hat{V}_I^*$ = 9.13x10^{-4} m^3/kg

$\hat{V}_m^*$ = 8.22x10^{-4} m^3/kg

Contd...b

Appendix II (contd... b)

$\hat{V}_p^*$ = 7.70×10^{-4} m^3/kg

M_{jp} = 0.18781 kg/mol

γ = 1

$V_{fm} = 0.149 + 2.9 \times 10^{-4} \left[T(K) - 273.1 \right]$

$V_{fp} = 0.0194 + 1.3 \times 10^{-4} \left[T(K) - 273.1 - 105 \right]$;
for $T < (105+273.1)$ K

Mark-Houwink Constants for Intrinsic Viscosity (see Eq. 29, App. I)

K = 6.75×10^{-6} m^3/kg

a = 0.72

K and a assumed to be (almost) independent of T

Parameters for the Adapted Lyons-Tobolsky Equation (Eq. 28, App. I)

$k_H = - d_1 + d_2 T$

$d_1 = 0.3118$; $d_2 = 9.93 \times 10^{-4}$ K^{-1} (this work)

b = $- 3.5 \times 10^{-3}$ m^3/kg (assumed independent of T)

$\eta_{sol} = \exp (- 0.099 + 496/T) / T^{1.5939}$ Pa-s (Ref. 5)

Correlations Used For Curve - Fitting

$\log_{10} [\theta_t(T), s] = a_1 - a_2(1/T) + a_3(1/T^2)$

$\log_{10} [\theta_p(T), s] = b_1 - b_2(1/T) + b_3(1/T^2)$

$\log_{10} [10^3 \theta_f(T), m^3 mol^{-1}] = c_1 - c_2(1/T) + c_3(1/T^2)$

Contd....c

Appendix II (contd... c)

$a_1 = 1.2408 \times 10^2$; $a_2 = 1.0314 \times 10^5$; $a_3 = 2.2735 \times 10^7$

$b_1 = 8.0593 \times 10^1$; $b_2 = 7.5 \times 10^4$; $b_3 = 1.765 \times 10^7$

$c_1 = 2.016 \times 10^2$; $c_2 = 1.455 \times 10^5$; $c_3 = 2.70 \times 10^7$ (this work)

APPENDIX III

VISCOSITY OF NONREACTING MMA - PMMA SYSTEMS[21]

No.	Conc. of polymer % by weight	T, °C	η, Poise
1	38.87	50	2800
2	38.87	70	2500
3	31.60	50	200
4	31.60	70	120
5	20.23	50	6.5
6	20.23	70	2.6

Since M_w were not measured, these were obtained by computation, as values corresponding to a reacting system at the same T and polymer concentration; $[I]_o$ = 15.48 mol/m^3.